iScience

CellPress
OPEN ACCESS

Article

Glutamine promotes human CD8$^+$ T cells and counteracts imiquimod-induced T cell hyporesponsiveness

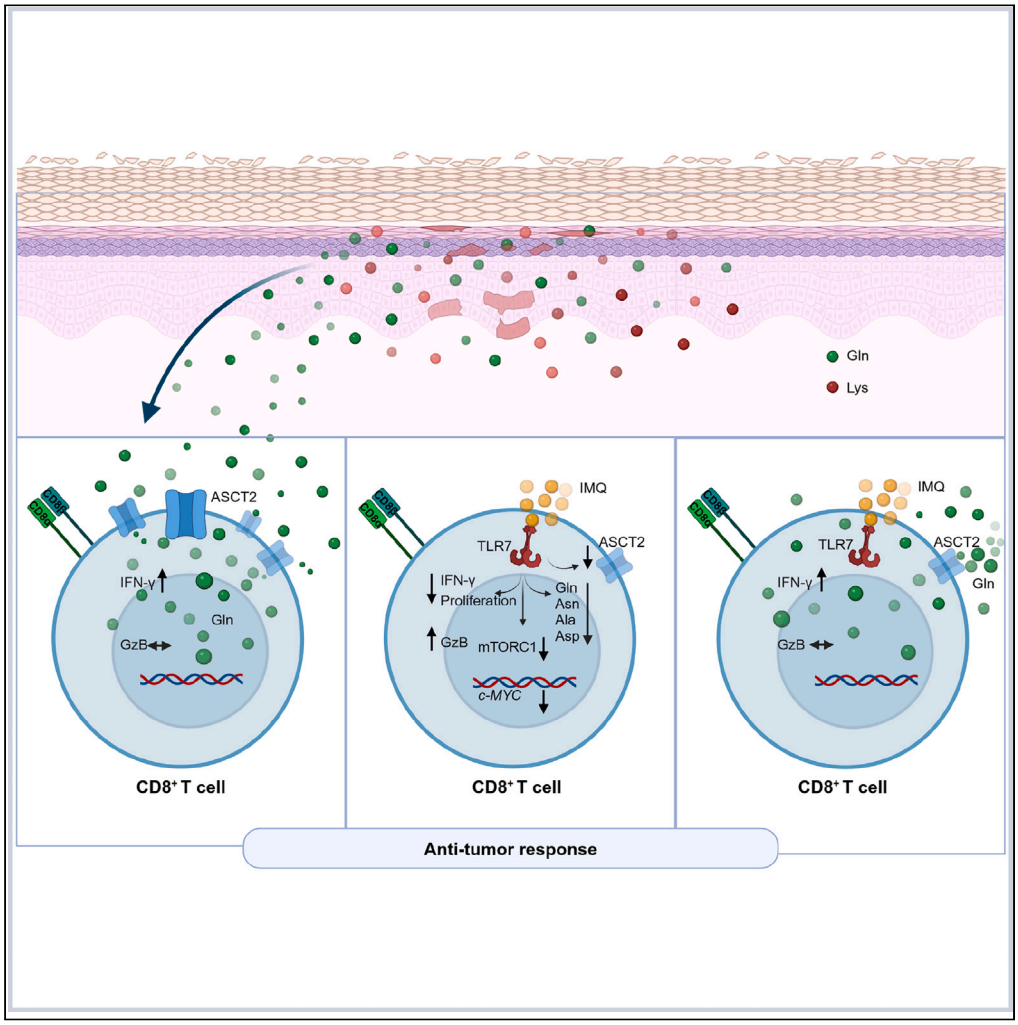

Luisa Bopp, Maria Lopéz Martinez, Clara Schumacher, ..., Susanne Brodesser, Ramon I. Klein Geltink, Mario Fabri

mario.fabri@uk-koeln.de

Highlights

Gln is an abundant extracellular amino acid in cutaneous human (pre)-cancer

Gln enhances IFN-γ production by human CD8$^+$ T cells

Imiquimod perturbs CD8$^+$ T cell AA metabolism, IFN-γ production, and proliferation

Gln is sufficient to promote IFN-γ production in imiquimod-treated CD8$^+$ T cells

Bopp et al., iScience 27, 109767
May 17, 2024 © 2024 The Author(s). Published by Elsevier Inc.
https://doi.org/10.1016/j.isci.2024.109767

iScience

CellPress
OPEN ACCESS

Article

Glutamine promotes human CD8$^+$ T cells and counteracts imiquimod-induced T cell hyporesponsiveness

Luisa Bopp,[1] Maria Lopéz Martinez,[1] Clara Schumacher,[1] Robert Seitz,[1] Manuel Huerta Arana,[1] Henning Klapproth,[1] Dominika Lukas,[1] Ju Hee Oh,[2,3] Daniela Neumayer,[1] Jan W. Lackmann,[4] Stefan Mueller,[5] Esther von Stebut,[1] Bent Brachvogel,[5,6,7,8] Susanne Brodesser,[8] Ramon I. Klein Geltink,[2,3] and Mario Fabri[1,5,9,*]

SUMMARY

T cells protect tissues from cancer. Although investigations in mice showed that amino acids (AA) critically regulate T cell immunity, this remains poorly understood in humans. Here, we describe the AA composition of interstitial fluids in keratinocyte-derived skin cancers (KDSCs) and study the effect of AA on T cells using models of primary human cells and tissues. Gln contributed to ~15% of interstitial AAs and promoted interferon gamma (IFN-γ), but not granzyme B (GzB) expression, in CD8$^+$ T cells. Furthermore, the Toll-like receptor 7 agonist imiquimod (IMQ), a common treatment for KDSCs, down-regulated the metabolic gatekeepers *c-MYC* and mTORC1, as well as the AA transporter ASCT2 and intracellular Gln, Asn, Ala, and Asp in T cells. Reduced proliferation and IFN-γ expression, yet increased GzB, paralleled IMQ effects on AA. Finally, Gln was sufficient to promote IFN-γ-production in IMQ-treated T cells. Our findings indicate that Gln metabolism can be harnessed for treating KDSCs.

INTRODUCTION

The ability of CD8$^+$ T cells to fight *in situ* and invasive cancer is pivotal to human skin homeostasis. Amino acids (AA) constitute key nutrients not only for tumor cells but also for T cells. They have essential roles in numerous cellular pathways, including activation of key signaling cascades, building blocks for protein synthesis, energy regeneration, redox homeostasis, and posttranscriptional modifications. It has become increasingly clear that AA support T cell function in cancer immunity.[1–10] Meanwhile, competition for nutrients between tumor cells and immune cells shapes the functionality of immune cell subsets in tissues,[2,5] and increasing evidence shows that the composition and quantity of intracellular and extracellular AA pools determines T cell fate and function.[1–10] Although the vast majority of evidence comes from investigations in mouse models, there is limited knowledge regarding AA availability and those factors regulating AA utilization by human CD8$^+$ T cells in skin malignancies.

Basal cell carcinoma (BCC) and squamous cell carcinoma (SCC) constitute keratinocyte-derived skin cancers (KDSCs), which, in sum, represent the most common human cancer.[11] At an early stage, KDSCs show a slowly progressive course. Moreover, the sequential development from pre-cancer lesions, termed actinic keratosis, to invasive cancer is highly characteristic for SCC.[12] In early KDSCs, imiquimod (IMQ), a synthetic Toll-like receptor 7 (TLR7) agonist, constitutes a frequently used destructive local therapy.[12,13] Although keratinocytes do not express TLR7,[14–16] the TLR7-mediated activation of plasmacytoid dendritic cells (pDCs) results in the induction of a strong inflammatory response.[17] Meanwhile, we recently showed that a coordinated expression of AA transporters and their function plays an essential role in the TLR-mediated activation of human pDCs.[18] Ultimately, the innate inflammatory response induced in IMQ-treated skin triggers the recruitment of effector T cells, among which CD8$^+$ T cells are of special importance for achieving cancer control.[19,20] Like pDCs, T cells express TLR7 and directly respond to its activation.[21]

In this project, we studied the role of AA in regulating T cell responses in the context of KDSCs using models of primary human cells and tissues. We found that, next to Lys, Gln represents the second most abundant AA in human actinic keratosis and established KDSCs.

[1]Department of Dermatology and Venereology, University of Cologne, Faculty of Medicine, and University Hospital of Cologne, Cologne, Germany
[2]BC Children's Hospital Research Institute, Vancouver, BC, Canada
[3]University of British Columbia, Vancouver, BC, Canada
[4]CECAD Cluster of Excellence, Faculty of Mathematics and Natural Sciences, University of Cologne, Cologne, Germany
[5]Center for Molecular Medicine Cologne (CMMC), Medical Faculty, University of Cologne, Cologne, Germany
[6]Department of Pediatrics and Adolescent Medicine, Experimental Neonatology, Medical Faculty and University Hospital Cologne, University of Cologne, Cologne, Germany
[7]Center for Biochemistry, Medical Faculty and University Hospital Cologne, University of Cologne, Cologne, Germany
[8]University of Cologne, Faculty of Medicine and University Hospital of Cologne, Cluster of Excellence Cellular Stress Responses in Aging-associated Diseases (CECAD), Cologne, Germany
[9]Lead contact
*Correspondence: mario.fabri@uk-koeln.de
https://doi.org/10.1016/j.isci.2024.109767

This is an open access article under the CC BY-NC license (http://creativecommons.org/licenses/by-nc/4.0/).

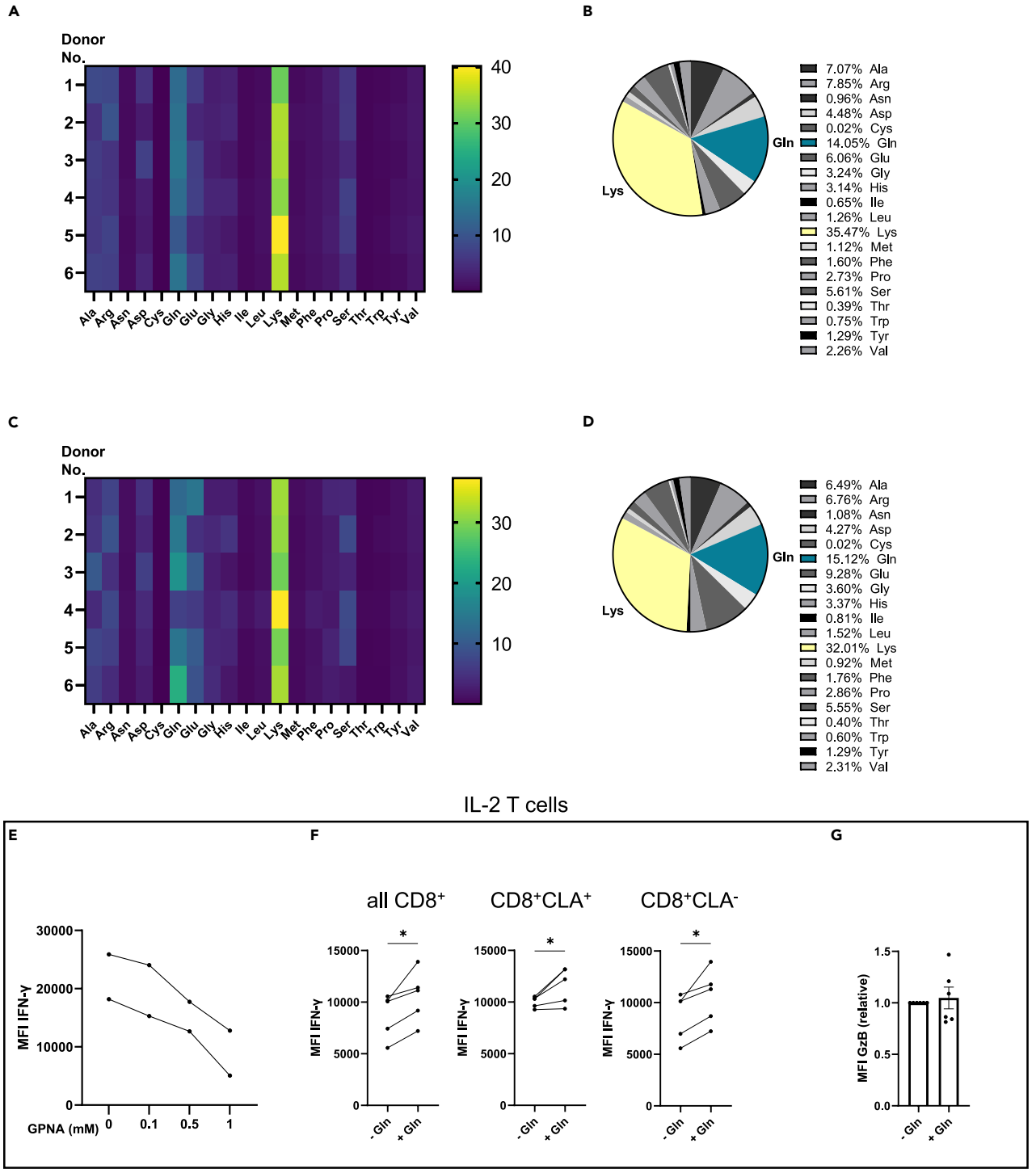

Figure 1. Gln supports IFN-γ production by human CD8⁺ T cells

Proteinogenic AA in interstitial tissue fluids of freshly excised biopsies from (A–B) actinically damaged skin and (C–D) KDSCs (each $n = 6$) were quantified by mass spectrometry.

(A and C) Heatmap plot showing 20 endogenous AA in six individual patients.

(B and D) Pie chart showing the relative contribution of individual AA to the complete pool of 20 AA detected (mean of the $n = 6$).

(E) $CD8^+$ IL-2 T cells were incubated with different concentrations of GPNA for 21 h. IFN-γ expression was measured by flow cytometry after restimulation with PMA/ionomycin for 5 h.

CellPress
OPEN ACCESS

Figure 1. *Continued*

(F) IFN-γ expression was assessed by flow cytometry in $CD8^+$ IL-2 T cells cultured in Gln-free medium supplemented with 4 mM Gln or not for 21 h after restimulation with PMA/ionomycin for 5 h.

(G) IFN-γ expression after restimulation with PMA/ionomycin for 5 h and (H) GzB expression in $CD8^+$ IL-2 T cells cultured in Gln-free medium supplemented with 4 mM Gln or not for 21 h were measured by flow cytometry. *$p < 0.05$, **$p < 0.01$, ****$p < 0.0001$. All data are shown as mean ± SEM. AA, amino acids; CLA, cutaneous lymphocyte antigen; GPNA, L-γ-glutamyl-*p*-nitroanilide; GzB, granzyme B; KDSC, keratinocyte-derived skin cancer.

Consistent with previous findings in mice,[1,6,22] Gln supported production of interferon gamma (IFN-γ), a pivotal effector anti-tumor cytokine, in human $CD8^+$ T cells. However, Gln did not regulate granzyme B (GzB) expression in these cells. Furthermore, we investigated how IMQ shapes AA metabolism in human $CD8^+$ T cells. We found that T cells in human KDSCs express TLR7. IMQ down-regulated expression of the alanine serine cysteine transporter 2 (ASCT2, also known as SLC1A5), an important AA transporter in human peripheral blood and $CD8^+$ tumor-infiltrating T cells (T-TILs). Moreover, IMQ reduced intracellular levels of Gln and three other AA, namely Asn, Ala, and Asp, among which Gln, Asn, and Ala can be transported by ASCT2. The observed changes in AA in IMQ-treated $CD8^+$ T cells were linked to a reduced expression of IFN-γ and proliferation, a paradoxical effect that has been demonstrated for human $CD4^+$ T cells before.[21] GzB expression, in contrast, was not altered by IMQ treatment. Finally, we observed that Gln was sufficient to promote IFN-γ expression in IMQ-treated human $CD8^+$ T cells.

RESULTS

Gln promotes effector functions of human $CD8^+$ T cells

AA shape T cell responses,[1–10] but little is known about the AA composition in human tissues, such as the skin. This prompted us to investigate the AA microenvironment in (pre-) cancerous skin. Specifically, we measured proteinogenic AA in interstitial tissue fluids of freshly excised biopsies from actinically damaged human skin and established KDSCs using liquid chromatography/mass spectrometry. We calculated the relative proportion of individual AA (Figures 1A–1D). Our analyses did not detect significant AA differences between pre-cancer lesions and fully established tumors, which could suggest a similar AA microenvironment in both stages of cancer progression. Gln and Lys were the most abundant AA (relative contributions of 14.05% and 35.47% in pre-cancerous skin [Figures 1A and 1B] and 15.12% and 32.01% in established KDSCs [Figures 1C and 1D], respectively). Given that previous studies in murine models have demonstrated that Gln directly supports T cell effector functions,[1,6,22] we asked about the effect of Gln on human $CD8^+$ T cells. To approach this question, we used a model of primary blood-derived human $CD8^+$ T effector cells expanded with CD3/CD28/CD2 tetramers and interleukin-2 (IL-2) ($CD8^+$ IL-2 T cells). These cells were incubated with different concentrations of the Gln analogue L-γ-glutamyl-*p*-nitroanilide (GPNA), an inhibitor of central cellular glutamine transporters.[23,24] After incubating for 21 h, we restimulated T cells with phorbol 12-myristate 13-acetate (PMA)/ionomycin for 5 h and measured production of IFN-γ, a cytokine that is intimately linked to T cell anti-tumor functions.[25–27] We found that GPNA decreased IFN-γ production in a dose-dependent manner (Figure 1E). To further elaborate the role of Gln on T cell IFN-γ production, we cultured $CD8^+$ IL-2 T cells in Gln-free medium, which is lacking Gln, Arg, and Lys, yet otherwise containing a standard cell-culture AA composition. Specifically, $CD8^+$ IL-2 T cells were cultured in Gln-free medium supplemented with Gln for not over 21 h and then restimulated with PMA/ionomycin. $CD8^+$ IL-2 T cells cultured with Gln produced significantly more IFN-γ than control T cells (Figure 1F, $p < 0.01$). We also stained cells with a monoclonal antibody directed against the cutaneous lymphocyte-associated antigen (CLA), a marker for skin-homing T cells in peripheral blood.[19,20,28] We found that Gln supported IFN-γ production in both CLA^+ and CLA^- $CD8^+$ T cell fractions (Figure 1F, $p < 0.01$). In contrast to IFN-γ, GzB expression was not regulated by Gln in $CD8^+$ T cells (Figure 1G). In sum, our data demonstrate that Gln promotes IFN-γ expression in both CLA^- non-skin-homing and CLA^+ skin-homing $CD8^+$ T cells.

IMQ perturbs AA metabolism in T cells

AA and their transporters are crucially involved in the TLR9- and TLR7-mediated activation of pDCs.[18] Specifically, SLC3A2 (CD98), a chaperone of AA transporters belonging to the SLC family, and SLC7A5 (LAT1) prime pDCs for activation via TLR ligands. Subsequent stimulation with TLR9 or TLR7 agonists triggers SCL7A11 expression in pDCs, driving enhanced pro-inflammatory activation.[18] T cells express TLR7, as we and others have shown for peripheral blood T cells (Figure S1;[21]), and can directly respond to its activation.[21] Thus, we asked if IMQ regulates AA metabolism in T cells. We approached this question by analyzing intracellular levels of proteinogenic AA in IMQ-treated and control $CD8^+$ IL-2 T cells. Quantification of intracellular AA by mass spectrometry revealed significantly lower levels of intracellular Ala, Asn, Asp, and Gln and a significantly higher level of Pro in IMQ-treated $CD8^+$ IL-2 T cells (Figure 2A, $p < 0.01$, $p < 0.05$, $p < 0.0001$, and $p < 0.05$, respectively). All other proteinogenic AA were not significantly different (Figures 2A and S2).

The reduction in intracellular levels of several AA corroborated our idea that IMQ shapes AA metabolism in human T cells. Given that regulating the expression of metabolic enzymes and transporters constitutes a major determinant of cellular metabolic adaptations, we performed proteomics analyses to screen for differentially expressed proteins involved in AA metabolism in IMQ-treated versus control T cells. $CD8^+$ IL-2 T cells were cultured with and without IMQ, and total cellular proteins were extracted after 24 h. By mass spectrometry we detected 4,216 proteins. Applying a statistical cutoff of $p < 0.05$, we identified 64 significantly down- and 41 significantly upregulated proteins (Figure 2B; Table S1). Among these significantly regulated proteins, ASCT2 was downregulated by 50% in IMQ-treated as compared with control $CD8^+$ T cells (Figure 2C, $p < 0.01$). Meanwhile, the expression of another AA transporter (ASCT1), the AA transporter chaperon SLC3A2 and glutaminase, which is an amidohydrolase that generates Glu from Gln, were reduced in five out of six donors (Figure S3). We confirmed

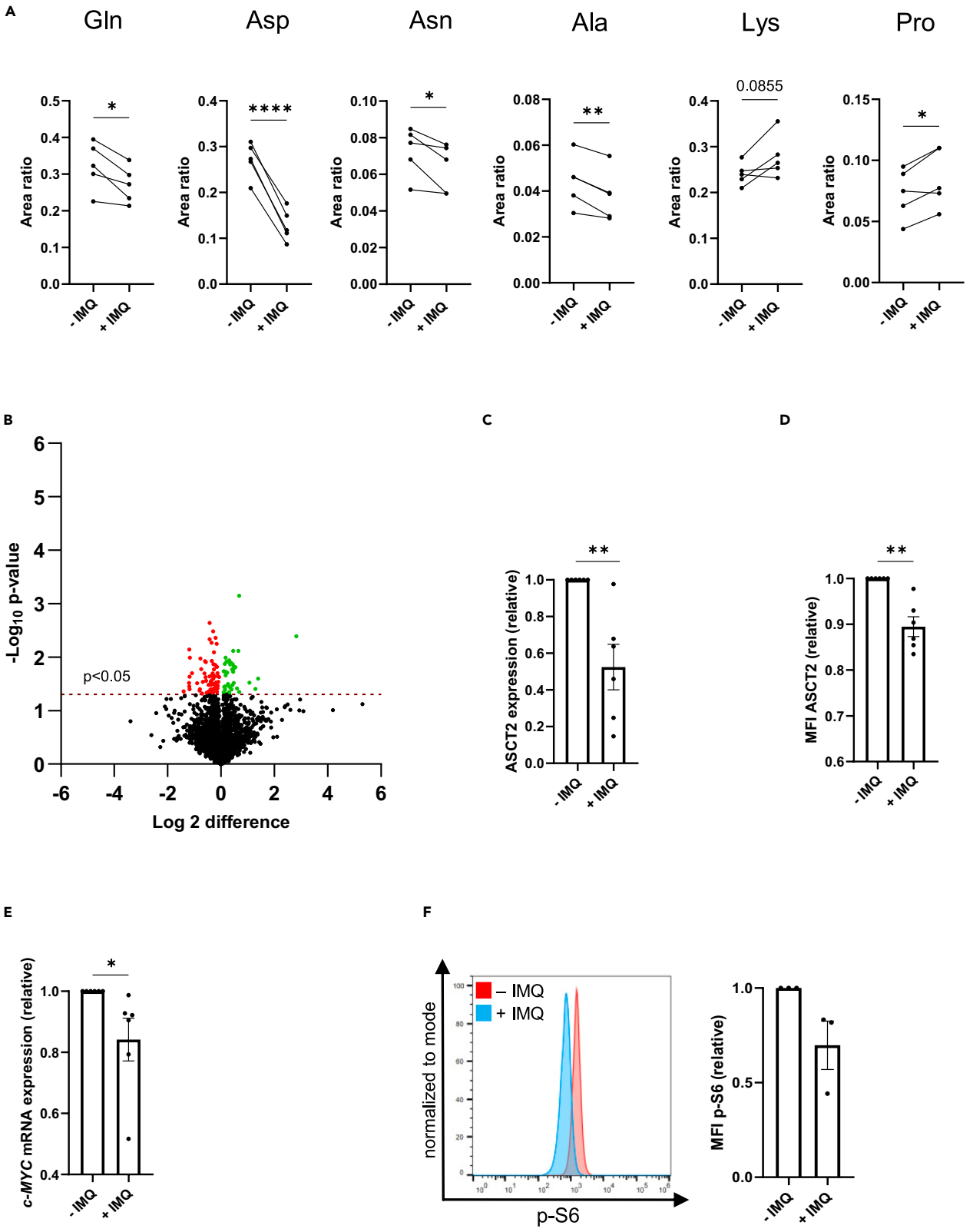
A
Gln
Asp
Asn
Ala
Lys
Pro
Area ratio
- IMQ
+ IMQ
*
****
0.0855
B
-Log10 p-value
Log 2 difference
p<0.05
C
ASCT2 expression (relative)
D
MFI ASCT2 (relative)
E
c-MYC mRNA expression (relative)
F
normalized to mode
– IMQ
+ IMQ
p-S6
MFI p-S6 (relative)

CellPress
OPEN ACCESS

Figure 2. IMQ perturbs AA metabolism in CD8$^+$ IL-2 T cells

CD8$^+$ IL-2 T cells were treated with IMQ for 21 h.

(A) Quantification of intracellular AA by mass spectrometry (n = 5).

(B and C) Proteomics analyses (n = 6). (B) Red dots in volcano plot indicate significantly downregulated, green dots significantly upregulated, and black dots indicate all other proteins. (C) Relative protein expression of ASCT2.

(D) ASCT2 expression measured by flow cytometry (n = 6).

(E) *c-MYC* mRNA expression evaluated by qPCR (n = 6).

(F) p-S6 expression measured by flow cytometry (n = 3). *$p < 0.05$, **$p < 0.01$, ****$p < 0.0001$. All data are shown as mean ± SEM. See also Figures S1–S3, and Table S1. AA, amino acids; ASCT, alanine serine cysteine transporter; IMQ, imiquimod; MFI, mean fluorescence intensity; p-S6, phospho-S6 ribosomal protein.

reduced expression of ASCT2 in blood-derived CD8$^+$ IL-2 T cells treated with IMQ vs. control cells at 21 h by flow cytometry (Figure 2D, $p < 0.01$). ASCT2 expression is regulated by the transcription factor *c-MYC*,[29] a downstream target of mammalian target of rapamycin complex 1 (mTORC1).[22,30] Consistent with a repressed ASCT2 expression, we found reduced mRNA expression of *c-MYC* in CD8$^+$ IL-2 T cells treated with IMQ for 21 h compared with the untreated counterparts (Figure 2E, $p < 0.05$). Moreover, flow cytometry experiments showed that expression of phospho-S6 ribosomal protein (p-S6), a marker for mTORC1-induced activation of the serine/threonine p70S6 kinase, was suppressed in CD8$^+$ IL-2 T cells (Figure 2F) upon IMQ treatment. In sum, our data show that IMQ repressed expression of ASCT2, its central upstream regulators *c-MYC* and mTORC1, as well as intracellular levels of several proteinogenic AA, indicating that IMQ alters AA homeostasis in human CD8$^+$ T cells.

To here, our investigations were based on peripheral-blood-derived T cells, yet we wondered if skin-derived T-TILs respond to IMQ treatment in the same way. Therefore, we established cell lines of T-TILs from human KDSC samples. We demonstrated that skin-derived T-TILs expressed TLR7 (Figure 3A). After treatment for 21 h with IMQ, CD8$^+$ T-TILs showed reduced expression of ASCT2 when compared with non-IMQ-treated controls (Figure 3B, $p < 0.05$), as well as p-S6 expression (Figure 3D, $p < 0.001$). Moreover, *c-MYC* mRNA levels (Figure 3C, $p < 0.0001$) were reduced after IMQ treatment for 4 h.

To investigate the effect of IMQ on T cells with regard to ASCT2 expression in a physiologic environment, we established a human skin cancer model for IMQ treatment. Therefore, full-thickness 8-mm punch biopsies from KDSCs were cut in half and placed each into culture plates. Cultures were left untreated or treated on day 1, 3, and 5 with IMQ, which corresponds to the standard treatment schedule in patients, who self-apply IMQ on day 1, 3, and 5 per week for few weeks. On day 7, we analyzed ASCT2 expression in CD8$^+$ T cells in this model. Flow cytometry staining showed that ASCT2 was downregulated by 73.3% in CD8$^+$ T cells treated with IMQ compared with control T cells (Figure 3E). In contrast, TLR7 expression was enhanced in the presence of IMQ (Figure 3F), which excludes a global suppressive effect on protein expression by IMQ in our model. Together, these data indicated a suppressive effect of IMQ on ASCT2 expression in CD8$^+$ T-TILs of human KDSCs.

IMQ reduces IFN-γ expression and proliferation in CD8$^+$ T cells

Given that metabolism and the function of T cells are fundamentally intertwined, we hypothesized that the altered AA metabolism in IMQ-treated CD8$^+$ T cells parallels changes in T cell function. To test this hypothesis, we measured IFN-γ production in both CD8$^+$ blood-derived IL-2 T cells as well as skin-derived T-TILs treated with IMQ for 21 h. We found that IMQ inhibits IFN-γ production in CLA$^+$ and CLA$^-$ blood-derived CD8$^+$ IL-2 T cells after restimulation with PMA/ionomycin when compared with non-IMQ-treated cells (Figure 4A, $p < 0.05$). Furthermore, IMQ reduced IFN-γ production by skin-derived T-TILs triggered by PMA/ionomycin (Figure 4B, $p < 0.001$) and also triggered by concomitant TCR activation with CD3/C28/CD2 activation tetramers during the 21-h culture period (Figure 4C, $p < 0.05$). In these experiments with human-skin-derived T-TILs, we additionally used CD39 co-staining, allowing the differentiation of CD39$^-$ bystander and CD39$^+$ tumor-reactive CD8$^+$ T cell subsets.[31,32] Subgating demonstrated a suppressive effect of IMQ on IFN-γ production in both CD8$^+$CD39$^-$ and CD8$^+$CD39$^+$ T cells (Figures 4B and 4C). In contrast to the observed repression of IFN-γ levels, GzB was enhanced by IMQ treatment, as demonstrated by flow cytometry and mass spectrometry analyses (Figures 4D and 4E, $p < 0.05$). Meanwhile, IL-10 and FoxP3 expression, markers of regulatory T cells, were sustained in T-TILs, in both CD8$^+$CD39$^-$ and CD8$^+$CD39$^+$ subsets after IMQ treatment (Figure S4, $p < 0.05$). Given that cytokine production has been linked to IMQ-triggered ROS production in several cell types,[33,34] we measured mitochondrial ROS using mitoSOX (staining mitochondrially accumulated O2·−), and cellular oxidative damage using cellROX in IMQ-treated CD8$^+$ IL-2 T cells and T-TILs. Nevertheless, we detected no changes in mitoSOX and cellROX in IMQ-treated IL-2 T cells and T-TILs when compared with corresponding control counterparts (Figure S5).

To test how IMQ regulates T cell proliferation, CD8$^+$ IL-2 T cells were labeled with 5(6)-carboxyfluorescein-diacetate-N-succinimidyl ester (CFSE) and treated with IMQ or not in the presence of IL-2 for 5 days. Flow cytometry analyses of CFSE dilution, without exogenous re-stimulation, revealed that IMQ reduced *ex vivo* T cell divisions (Figure 4F). Analyses of intracellular Ki-67 expression by flow cytometry, an additional method for measuring cell proliferation, confirmed reduced proliferation in IMQ-treated compared with control CD8$^+$ T cells after 21 h of culture (Figure 4G, $p < 0.01$). Suppressed proliferation was seen in both CLA$^+$ skin-homing and CLA$^-$ non-skin-homing CD8$^+$ T cell subsets (Figure 3G, both $p < 0.05$). To assess the effect of IMQ on proliferation of TCR-restimulated T cells, IL-2 T cells were reactivated using CD3/CD28/CD2 tetramers during IMQ treatment. After 21 h, IMQ-treated IL-2 T cells displayed reduced restimulation-mediated proliferation as compared with control cells (Figure 4H, $p < 0.01$). Again, a reduction in proliferation was seen in both the CLA$^+$ and CLA$^-$ fractions (Figure 4H, $p < 0.05$, and $p < 0.01$, respectively). Likewise, IMQ-treated skin-derived T-TILs cultured either with IL-2 alone (Figure 4I, $p < 0.01$) or cultured with IL-2 and reactivating CD3/CD28/CD2 tetramers (Figure 4J, $p < 0.01$) showed reduced Ki-67 expression after 21 h. Together, these

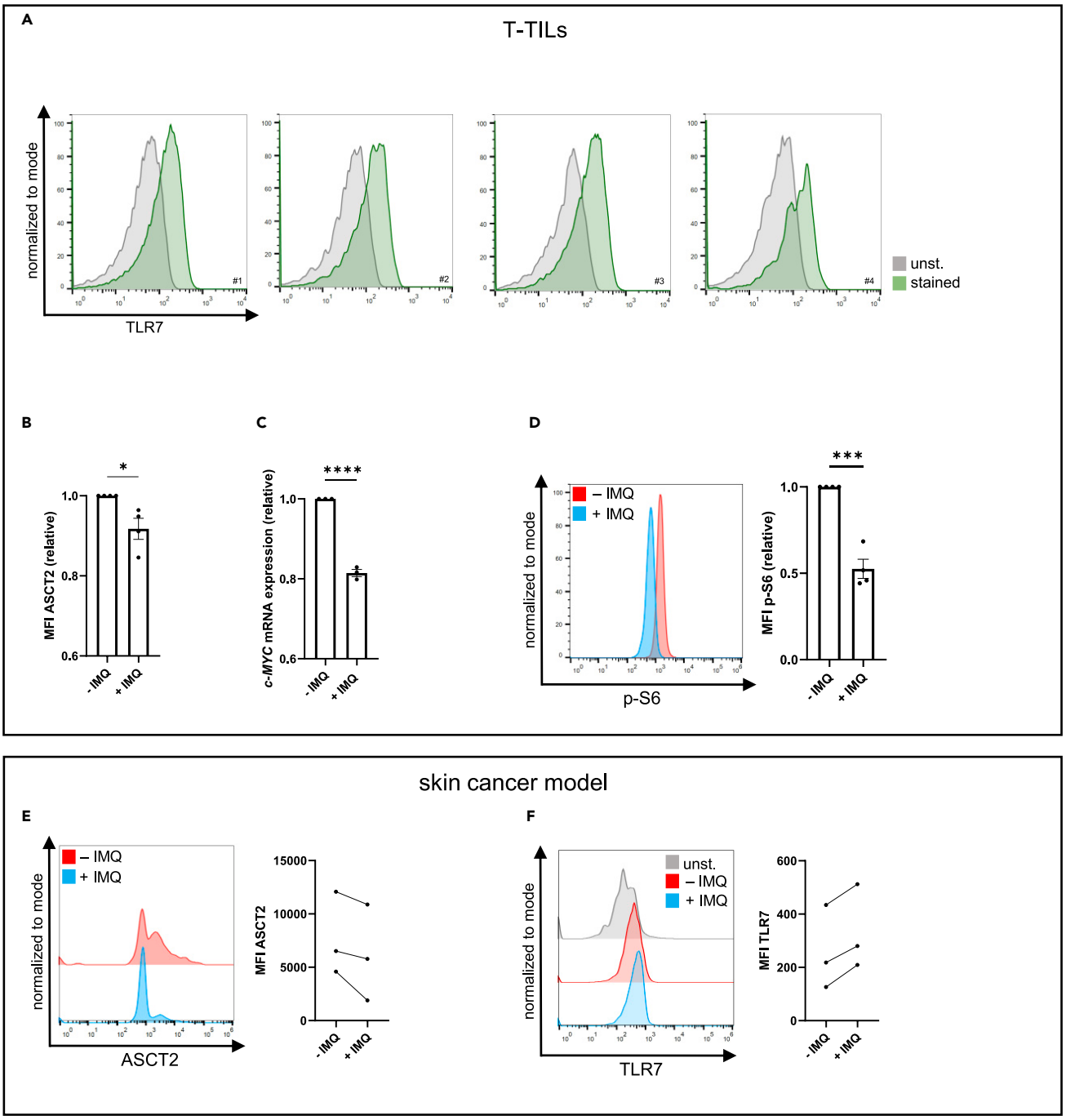

Figure 3. IMQ represses ASCT2 expression in CD8$^+$ T-TILs

(A) TLR7 expression in CD8$^+$ T-TIL lines assessed by flow cytometry (n = 4).

(B–D) CD8$^+$ T-TIL were treated with or without IMQ. (B) ASCT2 expression measured by flow cytometry after 21 h (n = 4). (C) *c-MYC* mRNA expression evaluated by qPCR after 4 h (n = 3). (D) p-S6 expression measured by flow cytometry after 21 h (n = 4).

(E and F) Full-thickness biopsies from KDSCs were cultured and left untreated or treated on day 1, 3, and 5 with IMQ. (E) ASCT2 and (F) TLR7 expression in CD8$^+$ T cells were determined by flow cytometry analyses on day 7. *$p < 0.05$, ***$p < 0.001$, ***$p < 0.0001$. All data are shown as mean ± SEM. ASCT, alanine serine cysteine transporter; IMQ, imiquimod; p-S6, phospho-S6 ribosomal protein; TLR7, toll-like receptor 7; unst., unstained.

CellPress
OPEN ACCESS

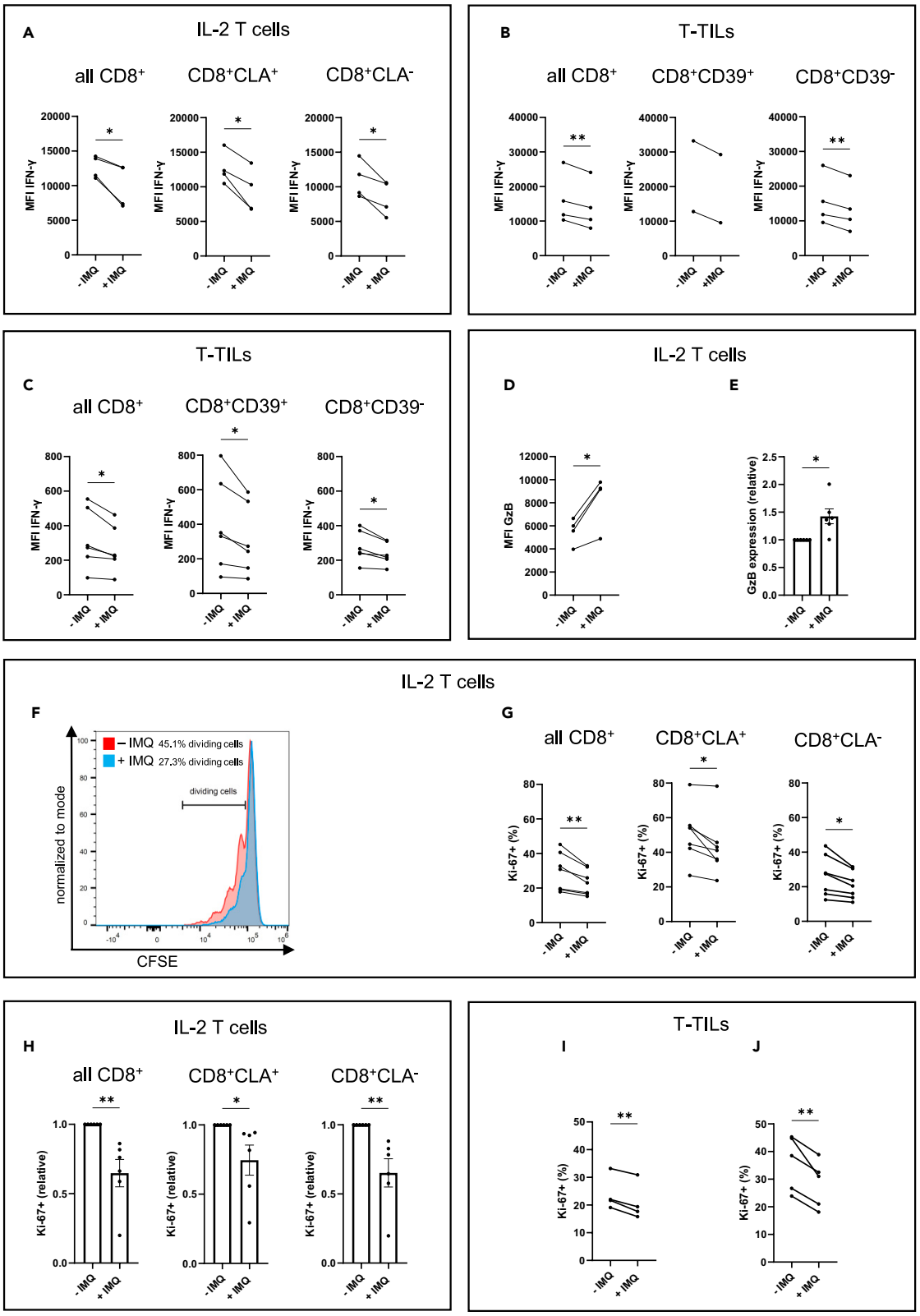

Figure 4. IMQ reduces IFN-γ expression and proliferation of CD8$^+$ T cells

T cells were treated with IMQ or not for 21 h (A–E and G–J) or for 5 days (F) and analyzed by flow cytometry (A–D and F–J) and proteomics (E). IFN-γ expression in (A) CD8$^+$ IL-2 T cells and (B) T-TILs reactivated with PMA/ionomycin and (C) in T-TILs reactivated with CD3/CD28/CD2 tetramers during IMQ treatment.
(D and E) GzB expression in CD8$^+$ IL-2 T cells.
(F) CD8$^+$ IL-2 T cells were analyzed for cell divisions using the CFSE dilution method. Representative histogram plot of one out of five donors.
(G) Ki-67 expression in CD8$^+$ IL-2 T cells cultured with IL-2 only (n = 7) or (H) reactivated with tetramers and IL-2 (n = 6).
(I) Ki-67 expression in CD8$^+$ T-TILs cultured with IL-2 only (n = 4) or (J) reactivated with tetramers and IL-2 (n = 5). *$p < 0.05$, **$p < 0.01$. All data are shown as mean ± SEM. See also Figures S4 and S5. CFSE, 5(6)-carboxyfluorescein-diacetate-N-succinimidyl ester; CLA, cutaneous lymphocyte antigen; GzB, granzyme B; IMQ, imiquimod; IFN-γ, Interferon-gamma; PMA, phorbol-12-myristat-13-acetat.

experiments showed that IMQ suppresses IFN-γ production and proliferation in blood-derived CD8$^+$ T cells, including those expressing the skin-homing marker CLA, as well as in skin-derived human T-TILs. These data demonstrate that IMQ induces CD8$^+$ T cell hyporesponsiveness in terms of proliferation and IFN-γ production.

Gln is sufficient to promote IFN-γ expression in IMQ-treated human CD8$^+$ T cells

Our data indicated that IMQ dysregulates AA metabolism, and this altered AA metabolism was paralleled by reduced IFN-γ production and proliferation. Given that intracellular Gln, Ala, Asn, and Asp were lowered upon IMQ-treatment (Figure 2A), we wondered if these AA alone or a pool of all four AA would counteract IFN-γ suppression in T cells treated with IMQ. We cultured IMQ-treated and untreated control CD8$^+$ IL-2 T cells in complete AA-free medium supplemented with either Gln, Ala, Asn, and Asp (each 2 mM) alone or a pool of all four AA for 21 h. After restimulation with PMA/ionomycin, IFN-γ expression was measured. We found that Gln alone and the pool of Gln, Ala, Asn, and Asp were sufficient in supporting IFN-γ production in control T cells and also in IMQ-treated CD8$^+$ IL-2 T cells (Figure 5A, $p < 0.01$, $p < 0.05$, and $p < 0.01$, $p < 0.001$, respectively). Asn and Ala alone also had some effect in non-IMQ-treated cells (Figure 5A, $p < 0.05$), yet this effect was absent in IMQ-treated cells. Furthermore, we found that Gln was as sufficient and as effective as the pool of the four AA to promote IFN-γ expression in T-TILs that were cultured in complete AA-free medium (Figure 5B). Moreover, Gln increased IFN-γ, but not GzB expression, in IMQ-treated CD8$^+$ IL-2 T cells in the Gln-free medium (also lacking Arg and Lys, yet otherwise containing a standard cell culture AA composition) (Figures 5C, $p < 0.01$, and 5D, respectively). Next, we investigated the effect of Gln on IFN-γ expression in IMQ-treated T cells in our skin cancer model. Halves of 8-mm punch biopsies were cultured in Gln-free medium with 2 mM Gln or not. Cultures were treated on day 1, 3, and 5 with IMQ together with 2 mM Gln or not. On day 6, cultures were harvested and T cells were re-stimulated with activation tetramers. After 21 h, flow cytometry analyses showed that IFN-γ expression was increased by Gln in CD8$^+$ T cells (Figure 5E, $p < 0.05$). In sum, these data demonstrate that Gln is sufficient to promote CD8$^+$ T cell effector responses, also in the context of IMQ-induced metabolic disturbances. The latter indicates that Gln can counteract the IMQ-induced IFN-γ hyporesponsiveness in human CD8$^+$ T cells.

DISCUSSION

In this study, we demonstrated a critical role of Gln in promoting IFN-γ production in human CD8$^+$ T cells. Furthermore, we showed that IMQ treatment of human CD8$^+$ T cells induces changes in AA metabolism. IMQ treatment resulted in a reduction of the intracellular AA Gln, Ala, Asn, and Asp. Moreover, the AA transporter ASCT2, involved in Gln, Ala, and Asn import, was reduced upon IMQ treatment. These changes were paralleled by a reduction in proliferation and IFN-γ expression, a paradoxical effect of IMQ, which was defined for CD4$^+$ T cells by others in the past.[21] Albeit we found reduced mTORC1 activity, which indicates profound metabolic adaptations of IMQ-treated T cells, the pool of four AA, Gln, Ala, Asn, and Asp, as well as Gln alone were sufficient in supporting IFN-γ production in IMQ-treated CD8$^+$ T cells. Together, these data define an important role of AA, in particular Gln, in T-cell-mediated immunity in KDSCs. Furthermore, our data indicate that Gln can improve T cell function and overcome paradoxical effects on T cell function in the context of IMQ-based therapies.

Out of the regulated AA in CD8$^+$ T cells after IMQ treatment, Gln, Ala, Asn, and Asp are intimately connected. Gln, Ala, and Asn are transported by ASCT2.[35,36] In T cells, ASCT2 represents a key transporter for Gln import.[6,37] Although Asp was the most strongly IMQ-regulated AA, Gln had the strongest functional impact on CD8$^+$ T cell IFN-γ production, as evident from experiments in which we limited AA availability. Furthermore, the Gln transport inhibitor GPNA reduced IFN-γ production by T cells. This is consistent with a large body of evidence that Gln is critical for T cell activation and effector function in mice.[1,6,22] Gln is a key fuel of the tricarboxylic acid cycle. Asp can be generated from the tricarboxylic acid cycle intermediate oxaloacetate via the Asp aminotransferase or hydrolyzed from Asn by asparaginase. Therefore, a reduction of Asp can, for instance, represent a secondary effect of Gln alterations, as the Asp generation from oxaloacetate represents a major contributor to AA homeostasis. In future studies, metabolic tracing experiments will be crucial for investigating the detailed metabolic events occurring under Gln substitution in IMQ-treated and untreated T cells, e.g., to which extent Gln is assimilated into the tricarboxylic acid cycle, contributes to enhance energy production and/or biosynthesis, or is directed to replenish Asp levels and other AA pools. Notably, Gln was sufficient to promote IFN-γ production in IMQ-treated cells, in which ASCT2 is downregulated. It is possible that increased substrate availability drives enhanced Gln uptake facilitated by remaining ASCT2 transporters and/or that other AA transporters, e.g., sodium-transported neutral AA transporter 1 or 2,[1,24,38] are important in promoting Gln uptake in this situation.

CellPress
OPEN ACCESS

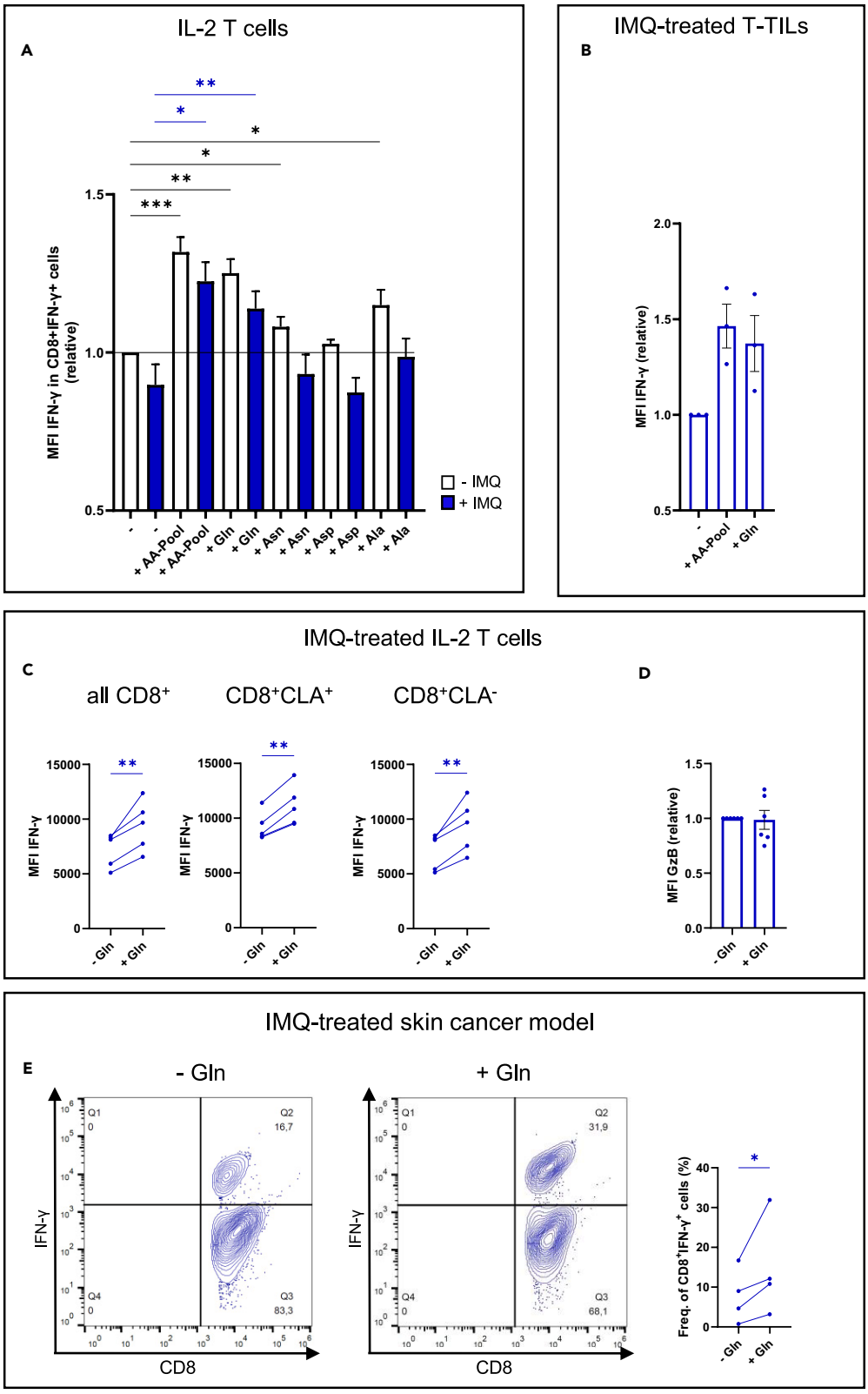

Figure 5. Gln is sufficient to promote IFN-γ expression in IMQ-treated CD8$^+$ T cells

(A) Control and IMQ-treated CD8$^+$ IL-2 T cells cultured in AA-free medium supplemented or not with Gln, Asn, Asp, or Ala alone or a pool of all four AA (each 2 mM) (n = 4). IFN-γ expression was assessed by flow cytometry.

(B) T-TILs were treated with IMQ and cultured in AA-free medium supplemented or not with Gln alone or a pool of all four AA over 21 h (n = 3). IFN-γ expression was assessed by flow cytometry.

(C and D) IMQ-treated CD8$^+$ IL-2 T cells were cultured in Gln-free medium supplemented with 4 mM Gln or not for 21 h. (C) IFN-γ expression and (D) GzB expression were measured by flow cytometry.

(E) Full-thickness biopsies from KDSCs were treated on day 1, 3, and 5 with IMQ together with or without Gln. After stimulation with activation tetramers on day 6 for 21 h, IFN-γ expression in CD8$^+$ T cells was determined by flow cytometry analyses on day 7 (n = 4).*$p < 0.05$, **$p < 0.01$ (in (E) values were log transformed to align data points to normal distribution). All data are shown as mean ± SEM. AA, amino acids; CLA, cutaneous lymphocyte antigen; T-TILs, tumor-infiltrating T lymphocytes.

Our finding that key metabolic regulators, mTORC1 and *c-MYC*, were regulated upon IMQ treatment suggests profound cellular metabolic adaptations in TLR7-agonist-treated T cells. This idea is supported by a previously published study on mouse and human T cells.[39] However, this recent study stands in contrast to our data as well as to other published data for CD4$^+$ T cells,[21] as it reports increased activation of CD8$^+$ T cells after TLR7/8-mediated activation, linked to enhanced glycolysis.[39] The exact reasons for these opposing results are not clear. However, the predominant use of mouse T cells in contrast to skin and blood human T cells, the predominant use of TLR7/8 agonist, opposed to the clinically used TLR7 agonist IMQ in our study, as well as the usage of a different IMQ concentration (1 μg/mL in the recent vs. 5 μg/mL in our study) might have contributed to this point.[21,39] Furthermore, differences in readouts for human T cells (early surface activation markers in the recent publication vs. T cell proliferation and IFN-γ production in our study) may well explain these apparent differences. Along these lines, in our model GzB expression was enhanced by IMQ treatment and was also not regulated by Gln. Of further relevance in this regard is a report showing that IMQ triggered perforin expression in CD8$^+$ T cells.[40] Together, these data suggest that the metabolic regulation of IFN-γ and other effector functions, such as GzB expression and perforin, substantially differ.

KDSCs, such as BCC and SCC, represent the most common human cancer worldwide, and their incidence is continuously increasing due to demographic change and sun exposure. From a clinical perspective, there is thus a need for improving local therapies against KDSCs. Albeit local treatments are often successful in pre-cancer and initial forms of KDSCs, recurrence is not uncommon and they fail to control more established cancer.[41–44] In a similar clinical condition, α-human papillomavirus (HPV)-induced peri- and intra-anal intraepithelial neoplasia (AIN), an anal pre-cancer, IMQ represents a standard, patient-applied topical treatment.[45,46] AIN causes significant morbidity in men who have sex with men living with HIV, and these patients suffer from high recurrence rates after treatment.[45,47,48] Particularly in the anal canal, where surgical therapy is limited due to the risk of scar contractures and anal stenosis, there is a clear need for effective topical therapies. Importantly, a central limiting side effect of IMQ both in skin and mucosal (pre-) cancer stems from the induction of overwhelming local and even systemic inflammation.[12,44,48] Noteworthy, IMQ is a potent trigger of innate inflammation, which is crucially mediated by TLR7 receptor activation in pDCs.[49–51] In a murine melanoma model, recruited pDCs have been shown to contribute directly to tumor killing via TNF-related apoptosis-inducing ligand and GzB secretion.[52] In this melanoma model, T cells were dispensable for anti-tumor effects.[52] Nevertheless, in human SCC treated with IMQ, the inflammatory responses readily result in T cell infiltration, and it is well accepted that T cells conduce to tumor control.[19,20] In any case, a simultaneously occurring suppressive effect of IMQ on effector functions of CD8$^+$ T cells, during the pDC-driven induction of innate immune responses, seems counterproductive. In the murine melanoma model, this potentially contributes to the diminished effect of T cells.[52] In humans, the idea of improving T cell responses by harnessing AA metabolism in the context of IMQ treatment, maybe even allowing to reduce IMQ doses and thus toxicity, constitutes an appealing therapeutic concept.

There is evidence that IMQ directly induces cell-cycle arrest/apoptosis in keratinocytes and different cancer cell lines *in vitro*,[52–57] as well as in murine keratinocytes and cancers *in vivo*.[52,56,57] This effect is partly dependent on TLR7-independent inflammasome activation.[57] Induction of apoptosis by IMQ in skin cancer cells can be mediated by ROS.[54,58] Nevertheless, in our experiments with IMQ-treated T cells, we did not detect an increased ROS production, suggesting that the observed effect of IMQ on T cells is not mediated via ROS induction. Furthermore, it has been shown that topical use of IMQ 5% cream *in vivo* induces a plethora of inflammatory responses by keratinocytes, which are largely TLR7-independent and even independent of the major active compound IMQ in the cream.[57] In contrast, IMQ-induced T cell un-responsiveness was previously shown to be TLR7-dependent.[21] Thus, future human studies testing the effect of AA on the interplay of innate and adaptive immune responses as well as cancer cells in IMQ-based treatment modalities and their clinical efficacy *in vivo* are warranted. Likewise, it will be interesting to also evaluate the effect of Gln and IMQ on HPV-specific immunity in AIN and other mucosal cancers. For α-HPV-induced mucosal cancers, a direct causal relationship between infection and cancer is accepted.[59,60] Albeit a link of β-HPV and SCC of the skin has been extensively documented, a causal relation awaits its definite approval.[61–63]

In conclusion, we define Gln as a crucial regulator of T cell immunity in the context of KDSCs. We demonstrated that IMQ-treated CD8$^+$ T cells show reduced mTORC1 activity and dysregulated AA metabolism. Nevertheless, Gln was sufficient to counteract the IMQ-induced reduction of IFN-γ production by CD8$^+$ T cells. Therefore, our study underscores the importance of Gln in supporting T cells in their anti-tumor function, defining Gln metabolism as a general therapeutic target. Finally, we deepen our molecular understanding of the complex, multifactorial effects of IMQ in anti-cancer treatments. Given that IMQ-induced paradoxical, suppressive effects on CD8$^+$ T cell responses are counterproductive in the context of immunologically driven cancer treatment, we provide a rationale for studying if

harnessing AA metabolism *in vitro* and *in vivo*, e.g., by high-dose exogenous AA, such as Gln, can improve effectiveness of IMQ-based cancer therapies.

Limitations of study

Our study has several limitations. Albeit a strength of our work is that we use primary human cells and human skin cancer samples, our investigations do not include *in vivo* animal models. Our study cannot identify potential differences in sex and gender due to small sample sizes. Because of a small sample size and the lack of matched healthy controls, our analyses on the AA composition in interstitial fluids do not allow us addressing general alterations in AA homeostasis in KDSCs. Furthermore, it remains to be determined, if reduced Gln levels in IMQ-treated cells represent a direct cause of ASCT2 downregulation.

STAR★METHODS

Detailed methods are provided in the online version of this paper and include the following:

- KEY RESOURCES TABLE
- RESOURCE AVAILABILITY
  - Lead contact
  - Materials availability
  - Data and code availability
- EXPERIMENTAL MODEL AND SUBJECT DETAILS
- METHOD DETAILS
  - T cell isolation, expansion and culture
  - Flow cytometry
  - Full-thickness human skin cancer model
  - Real-time quantitative PCR
  - Proteomic analyses using data independent acquisition using DIA-NN MBR
  - Quantification of AA
- QUANTIFICATION AND STATISTICAL ANALYSIS
  - Statistical analysis

SUPPLEMENTAL INFORMATION

Supplemental information can be found online at https://doi.org/10.1016/j.isci.2024.109767.

ACKNOWLEDGMENTS

This work was funded by the Deutsche Forschungsgemeinschaft (Bonn, Germany; SFB829, Projects B13 and Z4, as well as FA849/4-1). L.B. was supported by the Cologne Clinician Scientist Program (CCSP), Faculty of Medicine and University of Cologne, which is funded by the Deutsche Forschungsgemeinschaft (FI 773/15-1) and the Koeln Fortune Program/Faculty of Medicine, University of Cologne. D.L. was supported by the Koeln Fortune Program/Faculty of Medicine, University of Cologne. The proteomics experiment was supported by the large instrument grant INST 1856/71-1 FUGG for Orbitrap Exploris 480 by the Deutsche Forschungsgemeinschaft. E.v.S. received funding from the German Research Foundation (Project Number 318346496, SFB1292/2 TP15). R.I.K.G. is supported by a Michael Smith Health Research BC Scholar Award. The funders had no role in study design, data collection and analysis, decision to publish, or manuscript preparation. We thank Thomas Krieg for critical discussions, Paola Zigrino for assistance with the graphical abstract, Birgit Gathof for providing buffy coats, and all skin and blood donors.

AUTHOR CONTRIBUTIONS

Conceptualization: L.B. and M.F.; data curation: L.B. and M.F.; formal analysis: L.B., J.W.L., S.B., and M.F.; funding acquisition: L.B., D.L., E.v.S., R.I.K.G., and M.F.; investigation: L.B., M.L.M., C.S., R.S., M.H.A., H.K., S.B., R.I.K.G., and M.F.; methodology: L.B., J.H.O., D.L., S.B., B.B., S.M., J.W.L., R.I.K.G., and M.F.; project administration: L.B. and M.F.; resources: L.B., D.N., and M.F.; supervision: S.M., E.v.S., B.B., R.I.K.G., and M.F.; validation: L.B. and M.F.; visualization: L.B. and M.H.A.; writing—original draft preparation: L.B. and M.F.; writing—review and editing: L.B., M.L.M., C.S., R.S., M.H.A., H.K., D.L., J.H.O., D.N., J.W.L., S.M., E.v.S., B.B., S.B., R.I.K.G., and M.F.

DECLARATION OF INTERESTS

The authors have declared that no competing interests exist related to this study.

Received: May 10, 2023
Revised: February 24, 2024
Accepted: April 15, 2024
Published: April 18, 2024

REFERENCES

1. Carr, E.L., Kelman, A., Wu, G.S., Gopaul, R., Senkevitch, E., Aghvanyan, A., Turay, A.M., and Frauwirth, K.A. (2010). Glutamine Uptake and Metabolism Are Coordinately Regulated by ERK/MAPK during T Lymphocyte Activation. J. Immunol. *185*, 1037–1044. https://doi.org/10.4049/jimmunol.0903586.
2. Corrado, M., and Pearce, E.L. (2022). Targeting memory T cell metabolism to improve immunity. J. Clin. Invest. *132*, e148546. https://doi.org/10.1172/JCI148546.
3. Edwards, D.N., Ngwa, V.M., Raybuck, A.L., Wang, S., Hwang, Y., Kim, L.C., Cho, S.H., Paik, Y., Wang, Q., Zhang, S., et al. (2021). Selective glutamine metabolism inhibition in tumor cells improves antitumor T lymphocyte activity in triple-negative breast cancer. J. Clin. Invest. *131*, e140100. https://doi.org/10.1172/JCI140100.
4. Geiger, R., Rieckmann, J.C., Wolf, T., Basso, C., Feng, Y., Fuhrer, T., Kogadeeva, M., Picotti, P., Meissner, F., Mann, M., et al. (2016). L-Arginine Modulates T Cell Metabolism and Enhances Survival and Anti-tumor Activity. Cell *167*, 829–842.e13. https://doi.org/10.1016/j.cell.2016.09.031.
5. Kelly, B., and Pearce, E.L. (2020). Amino assets: how amino acids support immunity. Cell Metab. *32*, 154–175. https://doi.org/10.1016/j.cmet.2020.06.010.
6. Nakaya, M., Xiao, Y., Zhou, X., Chang, J.H., Chang, M., Cheng, X., Blonska, M., Lin, X., and Sun, S.C. (2014). Inflammatory T cell responses rely on amino acid transporter ASCT2 facilitation of glutamine uptake and mTORC1 kinase activation. Immunity *40*, 692–705. https://doi.org/10.1016/j.immuni.2014.04.007.
7. Ron-Harel, N., Ghergurovich, J.M., Notarangelo, G., LaFleur, M.W., Tsubosaka, Y., Sharpe, A.H., Rabinowitz, J.D., and Haigis, M.C. (2019). T Cell Activation Depends on Extracellular Alanine. Cell Rep. *28*, 3011–3021.e4. https://doi.org/10.1016/j.celrep.2019.08.034.
8. Sugiura, A., and Rathmell, J.C. (2018). Metabolic Barriers to T Cell Function in Tumors. J. Immunol. *200*, 400–407. https://doi.org/10.4049/jimmunol.1701041.
9. Wang, W., and Zou, W. (2020). Amino Acids and Their Transporters in T Cell Immunity and Cancer Therapy. Mol. Cell *80*, 384–395. https://doi.org/10.1016/j.molcel.2020.09.006.
10. Wu, J., Li, G., Li, L., Li, D., Dong, Z., and Jiang, P. (2021). Asparagine enhances LCK signalling to potentiate CD8+ T-cell activation and anti-tumour responses. Nat. Cell Biol. *23*, 75–86. https://doi.org/10.1038/s41556-020-00615-4.
11. Global Burden of Disease Cancer Collaboration, Fitzmaurice, C., Abate, D., Abbasi, N., Abbastabar, H., Abd-Allah, F., Abdel-Rahman, O., Abdelalim, A., Abdoli, A., Abdollahpour, I., et al. (2019). Global, regional, and national cancer incidence, mortality, years of life lost, years lived with disability, and disability-Adjusted life-years for 29 cancer groups, 1990 to 2017: A systematic analysis for the global burden of disease study. JAMA Oncol. *5*, 1749–1768. https://doi.org/10.1001/jamaoncol.2019.2996.
12. Gilchrest, B.A. (2021). Actinic Keratoses: Reconciling the Biology of Field Cancerization with Treatment Paradigms. J. Invest. Dermatol. *141*, 727–731. https://doi.org/10.1016/j.jid.2020.09.002.
13. Persaud, A., and Lebwohl, M. (2002). Imiquimod cream in the treatment of actinic keratoses. J. Am. Acad. Dermatol. *47*, S236–S239. https://doi.org/10.1067/mjd.2002.126581.
14. Köllisch, G., Kalali, B.N., Voelcker, V., Wallich, R., Behrendt, H., Ring, J., Bauer, S., Jakob, T., Mempel, M., and Ollert, M. (2005). Various members of the Toll-like receptor family contribute to the innate immune response of human epidermal keratinocytes. Immunology *114*, 531–541. https://doi.org/10.1111/j.1365-2567.2005.02122.x.
15. Lebre, M.C., Van Der Aar, A.M.G., Van Baarsen, L., Van Capel, T.M.M., Schuitemaker, J.H.N., Kapsenberg, M.L., and De Jong, E.C. (2007). Human keratinocytes express functional toll-like receptor 3, 4, 5, and 9. J. Invest. Dermatol. *127*, 331–341. https://doi.org/10.1038/sj.jid.5700530.
16. Rattay, S., Hufbauer, M., Hagen, C., Putschli, B., Coch, C., Akgül, B., and Hartmann, G. (2022). Human Beta Papillomavirus Type 8 E1 and E2 Proteins Suppress the Activation of the RIG-I-like Receptor MDA5. Viruses *14*. Viruses *14*, 1361. https://doi.org/10.3390/v14071361.
17. Stary, G., Bangert, C., Tauber, M., Strohal, R., Kopp, T., and Stingl, G. (2007). Tumoricidal activity of TLR7/8-activated inflammatory dendritic cells. J. Exp. Med. *204*, 1441–1451. https://doi.org/10.1084/jem.20070021.
18. Grzes, K.M., Sanin, D.E., Kabat, A.M., Stanczak, M.A., Edwards-Hicks, J., Matsushita, M., Hackl, A., Hässler, F., Knoke, K., Zahalka, S., et al. (2021). Plasmacytoid dendritic cell activation is dependent on coordinated expression of distinct amino acid transporters. Immunity *54*, 2514–2530.e7. https://doi.org/10.1016/j.immuni.2021.10.009.
19. Huang, S.J., Hijnen, D., Murphy, G.F., Kupper, T.S., Calarese, A.W., Mollet, I.G., Schanbacher, C.F., Miller, D.M., Schmults, C.D., and Clark, R.A. (2009). Imiquimod enhances ifn-γ production and effector function of T cells infiltrating human squamous cell carcinomas of the skin. J. Invest. Dermatol. *129*, 2676–2685. https://doi.org/10.1038/jid.2009.151.
20. Clark, R.A., Huang, S.J., Murphy, G.F., Mollet, I.G., Hijnen, D., Muthukuru, M., Schanbacher, C.F., Edwards, V., Miller, D.M., Kim, J.E., et al. (2008). Human squamous cell carcinomas evade the immune response by down-regulation of vascular E-selectin and recruitment of regulatory T cells. J. Exp. Med. *205*, 2221–2234. https://doi.org/10.1084/jem.20071190.
21. Dominguez-Villar, M., Gautron, A.S., De Marcken, M., Keller, M.J., and Hafler, D.A. (2015). TLR7 induces anergy in human CD4+ T cells. Nat. Immunol. *16*, 118–128. https://doi.org/10.1038/ni.3036.
22. Sinclair, L.V., Rolf, J., Emslie, E., Shi, Y.B., Taylor, P.M., and Cantrell, D.A. (2013). Control of amino-acid transport by antigen receptors coordinates the metabolic reprogramming essential for T cell differentiation. Nat. Immunol. *14*, 500–508. https://doi.org/10.1038/ni.2556.
23. Chiu, M., Sabino, C., Taurino, G., Bianchi, M.G., Andreoli, R., Giuliani, N., and Bussolati, O. (2017). GPNA inhibits the sodium-independent transport system l for neutral amino acids. Amino Acids *49*, 1365–1372. https://doi.org/10.1007/s00726-017-2436-z.
24. Bröer, A., Rahimi, F., and Bröer, S. (2016). Deletion of amino acid transporter ASCT2 (SLC1A5) Reveals an essential role for transporters SNAT1 (SLC38A1) and SNAT2 (SLC38A2) to sustain glutaminolysis in cancer cells. J. Biol. Chem. *291*, 13194–13205. https://doi.org/10.1074/jbc.M115.700534.
25. Dighe, A.S., Richards, E., Old, L.J., and Schreiber, R.D. (1994). Enhanced In Vivo Growth and Resistance to Rejection of Tumor Cells Expressing Dominant Negative IFNγ Receptors. Immunity *1*, 447–456.
26. Shankaran, V., Ikeda, H., Bruce, A.T., White, J.M., Swanson, P.E., Old, L.J., and Schreiber, R.D. (2001). IFNγ and lymphocytes prevent primary tumour development and shape tumour immunogenicity. Nature *410*, 1107–1111. https://doi.org/10.1038/35074122.
27. Street, S.E.A., Trapani, J.A., MacGregor, D., and Smyth, M.J. (2002). Suppression of lymphoma and epithelial malignancies effected by interferon γ. J. Exp. Med. *196*, 129–134. https://doi.org/10.1084/jem.20020063.
28. Fuhlbrigge, R.C., Kieffer, J.D., Armerding, D., and Kupper, T.S. (1997). Cutaneous lymphocyte antigen is a specialized form of PSGL-1 expressed on skin-homing T cells. Nature *389*, 978–981. https://doi.org/10.1038/40166.
29. Liu, P., Ge, M., Hu, J., Li, X., Che, L., Sun, K., Cheng, L., Huang, Y., Pilo, M.G., Cigliano, A., et al. (2017). A Functional Mammalian Target of Rapamycin Complex 1 Signaling Is Indispensable for c-Myc-Driven Hepatocarcinogenesis. Hepatology *66*, 161–181. https://doi.org/10.1002/hep.29183/suppinfo.
30. Wang, R., Dillon, C.P., Shi, L.Z., Milasta, S., Carter, R., Finkelstein, D., McCormick, L.L., Fitzgerald, P., Chi, H., Munger, J., and Green, D.R. (2011). The Transcription Factor Myc Controls Metabolic Reprogramming upon T Lymphocyte Activation. Immunity *35*, 871–882. https://doi.org/10.1016/j.immuni.2011.09.021.
31. Paijens, S.T., Vledder, A., de Bruyn, M., and Nijman, H.W. (2021). Tumor-infiltrating lymphocytes in the immunotherapy era. Cell. Mol. Immunol. *18*, 842–859. https://doi.org/10.1038/s41423-020-00565-9.

32. Simoni, Y., Becht, E., Fehlings, M., Loh, C.Y., Koo, S.L., Teng, K.W.W., Yeong, J.P.S., Nahar, R., Zhang, T., Kared, H., et al. (2018). Bystander CD8+ T cells are abundant and phenotypically distinct in human tumour infiltrates. Nature *557*, 575–579. https://doi.org/10.1038/s41586-018-0130-2.
33. Naik, E., and Dixit, V.M. (2011). Mitochondrial reactive oxygen species drive proinflammatory cytokine production. J. Exp. Med. *208*, 417–420. https://doi.org/10.1084/jem.20110367.
34. Peng, H.-Y., Lucavs, J., Ballard, D., Das, J.K., Kumar, A., Wang, L., Ren, Y., Xiong, X., and Song, J. (2021). Metabolic Reprogramming and Reactive Oxygen Species in T Cell Immunity. Front. Immunol. *12*, 652687. https://doi.org/10.3389/fimmu.2021.652687.
35. Song, W., Li, D., Tao, L., Luo, Q., and Chen, L. (2020). Solute carrier transporters: the metabolic gatekeepers of immune cells. Acta Pharm. Sin. B *10*, 61–78. https://doi.org/10.1016/j.apsb.2019.12.006.
36. Scalise, M., Pochini, L., Console, L., Losso, M.A., and Indiveri, C. (2018). The Human SLC1A5 (ASCT2) amino acid transporter: From function to structure and role in cell biology. Front. Cell Dev. Biol. *6*, 96. https://doi.org/10.3389/fcell.2018.00096.
37. Ren, W., Liu, G., Yin, J., Tan, B., Wu, G., Bazer, F.W., Peng, Y., and Yin, Y. (2017). Amino-acid transporters in T-cell activation and differentiation. Cell Death Dis. *8*, e2655. https://doi.org/10.1038/cddis.2017.
38. Mackenzie, B., and Erickson, J.D. (2004). Sodium-coupled neutral amino acid (System N/A) transporters of the SLC38 gene family. Pflügers Archiv *447*, 784–795. https://doi.org/10.1007/s00424-003-1117-9.
39. Li, Q., Yan, Y., Liu, J., Huang, X., Zhang, X., Kirschning, C., Xu, H.C., Lang, P.A., Dittmer, U., Zhang, E., and Lu, M. (2019). Toll-Like Receptor 7 Activation Enhances CD8+ T Cell Effector Functions by Promoting Cellular Glycolysis. Front. Immunol. *10*, 2191. https://doi.org/10.3389/fimmu.2019.02191.
40. Ambach, A., Bonnekoh, B., Nguyen, M., Schön, M.P., and Gollnick, H. (2004). Imiquimod, a Toll-like receptor-7 agonist, induces perforin in cytotoxic T lymphocytes in vitro. Mol. Immunol. *40*, 1307–1314. https://doi.org/10.1016/j.molimm.2004.01.002.
41. Sinx, K.A.E., Nelemans, P.J., Kelleners-Smeets, N.W.J., Winnepenninckx, V.J.L., Arits, A.H.M.M., and Mosterd, K. (2020). Surgery versus combined treatment with curettage and imiquimod for nodular basal cell carcinoma: One-year results of a noninferiority, randomized, controlled trial. J. Am. Acad. Dermatol. *83*, 469–476. https://doi.org/10.1016/j.jaad.2020.04.053.
42. Marks, R., Owens, M., and Walters, S.-A.; Australian Multi-Centre Trial Group (2004). Efficacy and Safety of 5% Imiquimod Cream in Treating Patients With Multiple Superficial Basal Cell Carcinomas. Arch. Dermatol. *140*, 1284–1285. https://doi.org/10.1001/archderm.140.10.1284-b.
43. Bath-Hextall, F., Ozolins, M., Armstrong, S.J., Colver, G.B., Perkins, W., Miller, P.S.J., and Williams, H.C.; Surgery versus Imiquimod for Nodular Superficial basal cell carcinoma SINS study group (2014). Surgical excision versus imiquimod 5% cream for nodular and superficial basal-cell carcinoma (SINS): A multicentre, non-inferiority, randomised controlled trial. Lancet Oncol. *15*, 96–105. https://doi.org/10.1016/S1470-2045(13)70530-8.
44. Hadley, G., Derry, S., and Moore, R.A. (2006). Imiquimod for actinic keratosis: Systematic review and meta-analysis. J. Invest. Dermatol. *126*, 1251–1255. https://doi.org/10.1038/sj.jid.5700264.
45. Wieland, U., Brockmeyer, N.H., Weissenborn, J.S., Hochdorfer, B., Stücker, M., Swoboda, J., Altmeyer, P., Pfister, H., and Kreuter, A. (2006). Imiquimod Treatment of Anal Intraepithelial Neoplasia in HIV-Positive Men. Arch. Dermatol. *142*. https://doi.org/10.1001/archderm.142.11.1438.
46. Sanclemente, G., Herrera, S., Tyring, S.K., Rady, P.L., Zuleta, J.J., Correa, L.A., He, Q., and Wolff, J.C. (2007). Human papillomavirus (HPV) viral load and HPV type in the clinical outcome of HIV-positive patients treated with imiquimod for anogenital warts and anal intraepithelial neoplasia. J. Eur. Acad. Dermatol. Venereol. *21*, 1054–1060. https://doi.org/10.1111/j.1468-3083.2007.02169.x.
47. Kreuter, A., Potthoff, A., Brockmeyer, N.H., Gambichler, T., Stücker, M., Altmeyer, P., Swoboda, J., Pfister, H., and Wieland, U.; German Competence Network HIV/AIDS (2008). Imiquimod leads to a decrease of human papillomavirus DNA and to a sustained clearance of anal intraepithelial neoplasia in HIV-infected men. J. Invest. Dermatol. *128*, 2078–2083. https://doi.org/10.1038/jid.2008.24.
48. Richel, O., de Vries, H.J.C., van Noesel, C.J.M., Dijkgraaf, M.G.W., and Prins, J.M. (2013). Comparison of imiquimod, topical fluorouracil, and electrocautery for the treatment of anal intraepithelial neoplasia in HIV-positive men who have sex with men: An open-label, randomised controlled trial. Lancet Oncol. *14*, 346–353. https://doi.org/10.1016/S1470-2045(13)70067-6.
49. Gibson, S.J., Lindh, J.M., Riter, T.R., Gleason, R.M., Rogers, L.M., Fuller, A.E., Oesterich, J.L., Gorden, K.B., Qiu, X., Mckane, S.W., et al. (2002). Plasmacytoid dendritic cells produce cytokines and mature in response to the TLR7 agonists, imiquimod and resiquimod. Cell. Immunol. *218*, 74–86. https://doi.org/10.1016/s0008-8749(02)00517-8.
50. Palamara, F., Meindl, S., Holcmann, M., Lührs, P., Stingl, G., and Sibilia, M. (2004). Identification and Characterization of pDC-Like Cells in Normal Mouse Skin and Melanomas Treated with Imiquimod. J. Immunol. *173*, 3051–3061. https://doi.org/10.4049/jimmunol.173.5.3051.
51. Urosevic, M., and Dummer, R. (2004). Role of Imiquimod in Skin Cancer Treatment. Am. J. Clin. Dermatol. *5*, 453–458.
52. Drobits, B., Holcmann, M., Amberg, N., Swiecki, M., Grundtner, R., Hammer, M., Colonna, M., and Sibilia, M. (2012). Imiquimod clears tumors in mice independent of adaptive immunity by converting pDCs into tumor-killing effector cells. J. Clin. Invest. *122*, 575–585. https://doi.org/10.1172/JCI61034.
53. Villamón, E., González-Fernández, J., Such, E., Cervera, J.V., Gozalbo, D., and Luisa Gil, M. (2018). Imiquimod inhibits growth and induces differentiation of myeloid leukemia cell lines. Cancer Cell Int. *18*, 15. https://doi.org/10.1186/s12935-018-0515-1.
54. Huang, S.-W., Chang, S.-H., Mu, S.-W., Jiang, H.-Y., Wang, S.-T., Kao, J.-K., Huang, J.-L., Wu, C.-Y., Chen, Y.-J., and Shieh, J.-J. (2016). Imiquimod activates p53-dependent apoptosis in a human basal cell carcinoma cell line. J. Dermatol. Sci. *81*, 182–191. https://doi.org/10.1016/j.jdermsci.2015.12.011.
55. Sohn, K.-C., Li, Z.J., Choi, D.-K., Zhang, T., Lim, J.W., Chang, I.-K., Hur, G.M., Im, M., Lee, Y., Seo, Y.-J., et al. (2014). Imiquimod Induces Apoptosis of Squamous Cell Carcinoma (SCC) Cells via Regulation of A20. PLoS One *9*, e95337. https://doi.org/10.1371/journal.pone.0095337.
56. HAN, J.-H., LEE, J., JEON, S.-J., CHOI, E.-S., CHO, S.-D., KIM, B.-Y., KIM, D.-J., PARK, J.-H., and PARK, J.-H. (2013). In vitro and in vivo growth inhibition of prostate cancer by the small molecule imiquimod. Int. J. Oncol. *42*, 2087–2093. https://doi.org/10.3892/ijo.2013.1898.
57. Walter, A., Schäfer, M., Cecconi, V., Matter, C., Urosevic-Maiwald, M., Belloni, B., Schönewolf, N., Dummer, R., Bloch, W., Werner, S., et al. (2013). Aldara activates TLR7-independent immune defence. Nat. Commun. *4*, 1560. https://doi.org/10.1038/ncomms2566.
58. Chang, S.-H., Lin, P.-Y., Wu, T.-K., Hsu, C.-S., Huang, S.-W., Li, Z.-Y., Liu, K.-T., Kao, J.-K., Chen, Y.-J., Wong, T.-W., et al. (2022). Imiquimod-induced ROS production causes lysosomal membrane permeabilization and activates caspase-8-mediated apoptosis in skin cancer cells. J. Dermatol. Sci. *107*, 142–150. https://doi.org/10.1016/j.jdermsci.2022.08.006.
59. zur Hausen, H. (1996). Papillomavirus infections — a major cause of human cancers. Biochim. Biophys. Acta *1288*, F55–F78. https://doi.org/10.1016/0304-419X(96)00020-0.
60. zur Hausen, H. (1977). Human Papillomaviruses and Their Possible Role in Squamous Cell Carcinomas. Curr. Top. Microbiol. Immunol. *78*, 1–30. https://doi.org/10.1007/978-3-642-66800-5_1.
61. Tampa, M., Mitran, C.I., Mitran, M.I., Nicolae, I., Dumitru, A., Matei, C., Manolescu, L., Popa, G.L., Caruntu, C., and Georgescu, S.R. (2020). The role of beta HPV types and HPV-associated inflammatory processes in cutaneous squamous cell carcinoma. J. Immunol. Res. *2020*, 5701639. https://doi.org/10.1155/2020/5701639.
62. Neagu, N., Dianzani, C., Venuti, A., Bonin, S., Voidăzan, S., Zalaudek, I., and Conforti, C. (2023). The role of beta-HPV in keratinocyte skin cancer development: A systematic review. J. Eur. Acad. Dermatol. Venereol. *37*, 40–46. https://doi.org/10.1111/jdv.18548.
63. Hufbauer, M., and Akgül, B. (2017). Molecular Mechanisms of Human Papillomavirus Induced Skin Carcinogenesis. Viruses *9*, 187. https://doi.org/10.3390/v9070187.
64. Quah, B.J.C., Warren, H.S., and Parish, C.R. (2007). Monitoring lymphocyte proliferation in vitro and in vivo with the intracellular fluorescent dye carboxyfluorescein diacetate succinimidyl ester. Nat. Protoc. *2*, 2049–2056. https://doi.org/10.1038/nprot.2007.296.
65. Fabri, M., Stenger, S., Shin, D.-M., Yuk, J.-M., Liu, P.T., Realegeno, S., Lee, H.-M., Krutzik, S.R., Schenk, M., Sieling, P.A., et al. (2011). Vitamin D Is Required for IFN-g-Mediated Antimicrobial Activity of Human Macrophages. Science translational medicine *3*. https://doi.org/10.1126/scitranslmed.3003045.
66. Knoke, K., Rongisch, R.R., Grzes, K.M., Schwarz, R., Lorenz, B., Yogev, N., Pearce, E.L., Pearce, E.J., Kofler, D.M., and Fabri, M. (2022). Tofacitinib Suppresses IL-10/IL-10R

Signaling and Modulates Host Defense Responses in Human Macrophages. J. Invest. Dermatol. *142*, 559–570.e6. https://doi.org/10.1016/j.jid.2021.07.180.

67. Chambers, M.C., MacLean, B., Burke, R., Amodei, D., Ruderman, D.L., Neumann, S., Gatto, L., Fischer, B., Pratt, B., Egertson, J., et al. (2012). A cross-platform toolkit for mass spectrometry and proteomics. Preprint *30*, 918–920. https://doi.org/10.1038/nbt.2377.
68. Demichev, V., Messner, C.B., Vernardis, S.I., Lilley, K.S., and Ralser, M. (2020). DIA-NN: neural networks and interference correction enable deep proteome coverage in high throughput. Nat. Methods *17*, 41–44. https://doi.org/10.1038/s41592-019-0638-x.
69. Tyanova, S., Temu, T., Sinitcyn, P., Carlson, A., Hein, M.Y., Geiger, T., Mann, M., and Cox, J. (2016). The Perseus computational platform for comprehensive analysis of (prote)omics data. Nat. Methods *13*, 731–740. https://doi.org/10.1038/nmeth.3901.
70. Wong, J.M.T., Malec, P.A., Mabrouk, O.S., Ro, J., Dus, M., and Kennedy, R.T. (2016). Benzoyl chloride derivatization with liquid chromatography-mass spectrometry for targeted metabolomics of neurochemicals in biological samples. J. Chromatogr. A *1446*, 78–90. https://doi.org/10.1016/j.chroma.2016.04.006.

CellPress
OPEN ACCESS

STAR★METHODS

KEY RESOURCES TABLE

REAGENT or RESOURCE	SOURCE	IDENTIFIER
Antibodies		
Alexa Fluor® 700 anti-human CD3 (clone HIT3a)	BioLegend	Product Code 300324, RRID:AB_493739
Brilliant Violet 605™ anti-human CD8 (clone SK1)	BioLegend	Product Code 344742, RRID:AB_2566513
FITC anti-human CD8 (clone BW135/80)	Miltenyi	Catalog No. 130-113-157
PerCP/Cyanine5.5 anti-human/mouse CLA (clone HEKA-452)	BioLegend	Product Code 321314, RRID:AB_2565766
Brilliant Violet 711 anti-human CD39 (clone A1)	BioLegend	Product Code 328228, RRID:AB_2632894
PE mouse anti-Ki67 (clone B56)	Becton Dickinson Biosciences	Catalog No. 556027, RRID:AB_2266296
PE/Cy7 anti-human IFN-γ (clone B27)	BioLegend	Product Code 506518
Allophycocyanin anti-human IL-10 (clone JES3-9D7)	BioLegend	Catalog No. 501410, RRID:AB_315176
PerCP-Cy5.5 FoxP3 (clone 236A/E7)	Becton Dickinson	Catalog No. 561493, RRID:AB_10714077
Unconjugated monoclonal rabbit anti-ASCT2 antibody (clone D7C12)	Cell Signaling Technologies	Catalog No. 8057, RRID:AB_10891440
Unconjugated polycloncal rabbit anti-Phospho-S6 Ribosomal Protein (Ser235/236) antibody	Cell Signaling Technologies	Catalog No. 2211, RRID:AB_331679
Goat anti-Rabbit IgG (H+L) Cross-Adsorbed Secondary Antibody, Alexa Fluor™ 488	Thermo Fisher Scientific	Catalog No. A-11034, RRID:AB_2576217
Anti-rabbit IgG (H+L), F(ab')2 Fragment (Alexa Fluor® 647 Conjugate)	Cell Signaling Technology	Product No. 4414S
5(6)-Carboxyfluorescein-diacetat-N-succinimidylester (CFSE)	Sigma-Aldrich	Product No. 21888
Biological samples		
Human blood (buffy coats from healthy blood donors)	Blood donor center, University of Cologne	N/A
Skin biopsies from patients with KDSC	Department of Dermatology and Venereology at the University of Cologne	N/A
Chemicals, peptides, and recombinant proteins		
CD8 MicroBeads, human	Miltenyi Biotec	Order No. 130-045-201
Human IL-2 IS research grade	Miltenyi Biotec	Order No. 130-097-743
ImmunoCult™ Human CD3/CD28/CD2 T Cell Activator	Stemcell Technologies	Catalog No. 10970
D-Glucose solution	Sigma-Aldrich	Product No. G8644
L-Glutamine solution	Sigma-Aldrich	Product No. G7513
L-Alanine	Sigma-Aldrich	Product No. A7469
L-Asparagine monohydrat	Roth	Product No. KK37.1
L-Aspartic Acid	Sigma-Aldrich	Product No. A7219
Imiquimod (R837)	InvivoGen	CAS No. 99011-78-6
GPNA (L-γ-Glutamyl-p-Nitroanilide)	Absource Diagnostics GmbH	Product No. S6670-0005
eBioscience™ Foxp3/Transcription Factor Staining Buffer Set	Thermo Fisher Scientific	Catalog No. 00-5523-00
Cytofix/Cytoperm Permeabilization Kit	BD Biosciences	Catalog No. 554714
FcR blocking reagent, human	Miltenyi Biotec	Order No. 130-059-901
Fixable Viability Dye eFluor™ 780	Invitrogen	Catalog No. 65-0865-14
mitoSOX™ red	Invitrogen	Catalog No. M36008
cellROX green	Invitrogen	Catalog No. C10444
eBioscience™ Brefeldin A-Lösung	ThermoFisher Scientific	Catalog No. 00-4506-51

(*Continued on next page*)

Continued

REAGENT or RESOURCE	SOURCE	IDENTIFIER
Phorbol 12-myristate 13-acetate (PMA)	Sigma Aldrich	CAS No. 16561-29-8
Ionomycin	Sigma Aldrich	SKU No. I9657
Critical commercial assays		
RNEasy Mini Kit	Qiagen	Catalog No. 74106
iScript™ cDNA Synthesis Kit	Bio-Rad Laboratories	Order No. 1708891
Hs_MYC_1_SQ QuantiTect Primer Assay	Qiagen	QT00035406
Deposited data		
Mass spectrometry proteomics data	This paper	ProteomeXchange Consortium: accession no. PXD038621 https://www.ebi.ac.uk/pride/
Software and algorithms		
FlowJo version 10.7.1	FlowJo	https://www.flowjo.com/
Prism 10.1.2 software	GraphPad	
Perseus 1.6.15	Perseus	https://www.maxquant.org/perseus/
MultiQuant 3.0.2 software	SCIEX	https://sciex.com/products/software/multiquant-software

RESOURCE AVAILABILITY

Lead contact

Further information and requests for resources and reagents should be directed to and will be fulfilled by the lead contact, Mario Fabri (mario.fabri@uk-koeln.de).

Materials availability

This study did not generate new unique reagents.

Data and code availability

- The mass spectrometry proteomics data are available under accession no. PXD038621 in the ProteomeXchange Consortium (https://www.ebi.ac.uk/pride/). All other data are included in this article and its Supplemental Materials.
- This paper does not report original code.
- Any additional information required to reanalyze the data reported in this paper is available from the lead contact upon request.

EXPERIMENTAL MODEL AND SUBJECT DETAILS

Punch biopsies from patients with established KDSCs, who underwent surgery for their tumors were collected at the Department of Dermatology and Venereology at the University of Cologne. We obtained tissue biopsies from n=9 SCCs, n=9 BCCs, n= 2 Morbus Bowen, and n=9 actinically damaged skin samples from 6 female and 13 male patients. The mean age of the patients was 73 years (range 31 – 89). The tissues were used for generation of human T-TIL lines, experiments with the human skin cancer model, and extraction of metabolites.

Human blood was collected from healthy blood donors at the blood donor center, University of Cologne. Age and sex of the blood donors were blinded to us. The blood was used to generate $CD8^+$ IL-2 T cell lines.

We did not perform sex-and-gender-based analyses. The availability of human samples is limited and our cohort size is too small to perform such analyses. In the experiments, in which we used buffy coats, we do not have, and are not allowed to have, any information on the gender and sex of the donors. We only included biopsies from white European patients, as they represent the main risk group for developing KDSCs and account for almost 100% of our patient cohorts.

This study was conducted according to the principles expressed in the Declaration of Helsinki and approved by the local Ethic Committee (*Ethikkommission*) of the University of Cologne (votes #08-144, #20-1082 and #19-1146). All donors provided written informed consent for the collection of blood and tissue and subsequent analyses.

METHOD DETAILS

T cell isolation, expansion and culture

IL-2 T cell lines were generated from buffy coats of healthy donors. Therefore, peripheral blood mononuclear cells were extracted by using Ficoll Paque. $CD8^+$ T cells were isolated from peripheral blood mononuclear cells through MidiMACS cell separation system using CD8 MicroBeads according to manufacturer's instructions.

T-TIL lines were generated out of 4-mm punch biopsies from patients with established KDSC and pre-cancer (n=3 SCCs, n= 4 BCCs, n=5 actinically damaged skin). Tissue pieces were placed into 48-well plates and incubated with 1 mL enriched medium (RPMI 1640 with L-glutamine, 1% sodium pyruvate, 1% penicillin/streptomycin, and 55 μmol/L 2-mercaptoethanol), and 10% human serum plus 10 U/mL IL-2 at 37°C, 5% CO2. After two days, 10 U/mL fresh IL-2 were added. On day 4, the tissue piece was removed, and the migrated T cells were collected and expanded.

For expansion, IL-2 T cell and T-TIL lines were stimulated with ImmunoCult™ Human CD3/CD28/CD2 T Cell Activator (T cell activation tetramers) for up to 36 hours in T cell enriched medium containing IL-2 according to the manufacturer's protocol. Enriched medium supplemented with IL-2 was replaced every third to fourth day. IMQ treatment experiments were performed in two-weeks-old T cell cultures. The concentration of IMQ was 5 μg/ml.

During IMQ treatment, T cells were maintained with 10% FCS and 10 U/ml IL-2 in regular RPMI medium or SILAC RPMI Flex Media (both Thermo Fisher Scientific) containing 10 mM glucose with or without Gln, or in AA-free Dulbecco's MEM complemented with individual AA, as indicated in figure legends. In Gln-supplementation experiments with complete AA-free Dulbecco's MEM 2 mM Gln were used, and in experiments with Gln-free SILAC RPMI Flex Media 4mM Gln were used. Because of the difference in the technical setup, IFN-γ expression was compared in $CD8^+$ IL-2 T cells cultured in Gln-free medium supplemented with either 2 or 4 mM Gln and no differences were found (data not shown).

Flow cytometry

The fluorochrome-conjugated monoclonal antibodies used for surface staining are found in the key features table. Staining was performed in FACS buffer for 20 min at 4°C. Dead cells were excluded by staining with Fixable Viability Dye and unspecific binding was blocked with FcR Blocking Reagent. After staining with surface markers and dyes, cells were fixed and permeabilized. For ASCT2 staining, eBioscience™ Foxp3/Transcription Factor Staining Buffer Set was used according to manufacturer's instructions. Cells were first stained with unconjugated anti-ASCT2 monoclonal antibody for 1 hour at room temperature (RT), and then with Alexa Fluor™ 488-conjugated IgG (H+L) secondary Ab for 30 min at RT. For Ki-67 and Foxp3 staining, eBioscience™ Foxp3/Transcription Factor Staining Buffer Set was used according to manufacturer's protocol. Cells were stained with anti-Ki-67 or anti-FoxP3 for 30 min at RT. For pS6-ribosomal protein staining, Cytofix/Cytoperm Permeabilization Kit was used. Cells were first stained with unconjugated polyclonal anti-pS6 Ab for 30 min at RT, and then with Alexa Fluor® 647-conjugated anti-IgG (H+L), F(ab')2 Fragment secondary Ab for 30 min at 4°C. For TLR7 and GzB staining, cells were fixed and permeabilized with Cytofix/Cytoperm Permeabilization Kit. Staining was performed with anti-TLR7- and anti-GzB-antibodies according to manufacturer's instructions.

For intracellular cytokine staining, cells were restimulated with 50 ng/mL PMA plus 0·5 μg/mL ionomycin for 5 hours in fresh medium or with T cell activation tetramers and IL-2 for 21 hours. Brefeldin A was added for the final 2·5 hours. After the boosting step, cells were fixed and permeabilized with Cytofix/Cytoperm Permeabilization Kit. Staining was performed with anti-IFN-γ and anti-IL-10 monoclonal antibodies. IFN-γ expression was evaluated by the MFI of IFN-γ in all $CD8^+$ T cells, when reactivated with T cell activation tetramers and IL-2, or in the IFN-γ^+ cells, when reactivated with PMA/ionomycin. IL-10 expression was evaluated by the MFI of IL-10 in all T cells. For analysis of T cell proliferation by means of CFSE staining, IL-2 T cells were stained with CFSE.[64] After five days, surface staining was performed and proliferation was assessed as the percentage of CFSE-negative cells (% dividing cells).

For evaluation of ROS, cells were stained with 2.5 μM mitoSOX red and 5 μM cellROX green (incubation for 30 minutes at 37°C) before surface staining.

For flow cytometry acquisition, cells were resuspended in FACS buffer and put on ice. Acquisition of cells was performed on an Attune NxT Flow Cytometer (Thermo Fisher Scientific). Data were analyzed using FlowJo software (Tree Star, Ashland OR).

Full-thickness human skin cancer model

For ASCT2 and TLR7 analyses, full-thickness 8-mm punch biopsies from KDSC (n=2 SCCs, n=1 BCC) were cut in half and placed each into 48-well plates containing 1 ml enriched medium and 10% human serum plus 10U/m IL-2. Cultures were treated with 5μg/ml IMQ or not on day 1, 3, and 5. In both conditions, cultures were supplemented with 10 U/ml IL-2 on day 1, 3, and 5. On day 7, the tumor piece was removed and ASCT2 and TLR7 expression was analyzed in migrated $CD8^+$ T cells by flow cytometry. For evaluation of T cell IFN-γ expression, 8-mm punch biopsies from KDSC (n=3 BCC, n=1 Morbus Bowen) were cut in half and placed each into 48-well plates containing 1 ml Gln-free RPMI1640 (Thermo Fisher Scientific) with 2mM Gln or not, and 10% human serum plus 10 U/m IL-2. Cultures were treated with 5 μg/ml IMQ on day 1, 3, and 5, and supplemented with 10 U/ml IL-2 and 2 mM Gln or not on day 1, 3, and 5. On day 6, migrated cells were washed, resuspended in fresh Gln-free media containing 10% human serum and IL-2 and stimulated with T cell activation tetramers over 21 hours. Brefeldin A was added for the final 2·5 hours. Then, cells were fixed and stained for IFN-γ (see above) after surface staining for CD3 and CD8 and permeabilisation/fixation with Cytofix/Cytoperm Permeabilization Kit.

Real-time quantitative PCR

mRNA was prepared from T cells using the RNEasy Mini Kit according to the manufacturer's instructions. cDNA was synthesized from mRNA using iScript cDNA Synthesis Kit and c-*MYC* mRNA levels were calculated by quantitative PCR as previously described.[65,66]

Proteomic analyses using data independent acquisition using DIA-NN MBR

For sample preparation, pellets were lysed in 8 M urea, reduced and alkylated with Dithiothreitol and Chloroacetamide (both from Sigma Aldrich), respectively, followed digestion with Lysyl Endopeptidase (Wako) and trypsin (Serva) overnight. Afterwards, samples were purified using self-packed styrenedivinyl benzene (SDB)-StageTips.

For data acquisition, samples were analyzed by the CECAD Proteomics Facility on an Orbitrap Exploris 480 mass spectrometer equipped with a FAIMS pro differential ion mobility device that was coupled to an UltiMate 3000 (all from Thermo Scientific). Samples were loaded onto a precolumn (Acclaim 5μm PepMap 300 μ Cartridge) for 2 min at 15 μl flow with eluent a (0·1% formic acid) before reverse-flushed onto an in-house packed analytical column (30 cm length, 75 μm inner diameter, filled with 2·7 μm Poroshell EC120 C18, Agilent). Peptides were chromatographically separated at a constant flow rate of 300 nL/min and the following gradient: initial 2% B (0·1% formic acid in 80 % acetonitrile), up to 6 % B in 1 min, up to 32% B in 72 min, up to 55% B within 7·0 min and up to 95% solvent B within 2·0 min, followed by column wash with 95% solvent B and reequilibration to initial condition. The FAIMS pro was operated at -50V compensation voltage and electrode temperatures of 99·5°C for the inner and 85°C for the outer electrode.

MS1 scans were acquired from 399 m/z to 1001 m/z at 15k resolution. Maximum injection time was set to 22 ms and the AGC target to 100%. MS2 scans ranged from 400 m/z to 1000 m/z and were acquired at 15 k resolution with a maximum injection time of 22 ms and an AGC target of 100%. DIA scans covering the precursor range from 400 - 1000 m/z and were acquired in 75 x 8 m/z staggered windows, resulting in nominal windows of 4 m/z after deconvolution using Proteowizard.[67] All scans were stored as centroid.

For processing, samples were analyzed in DIA-NN 1.8.[68] A human Swissprot canonical database (UP5640, downloaded 18/06/20) was used for library building with settings matching acquisition parameters and the match-between-runs function enabled. Here, samples are directly used to refine the library for a second search of the sample data. DIA-NN was run with the additional command line prompts "—report-lib-info" and "—relaxed-prot-inf". Further output settings were: filtered at 0·01 FDR, N-terminal methionine excision enabled, maximum number of missed cleavages set to 1, min peptide length set to 7, max peptide length set to 30, min precursor m/z set to 400, max precursor m/z set to 1000, cysteine carbamidomethylation enabled as a fixed modification. Afterwards, DIA-NN output was further filtered on library q-value and global q-value <= 0·01 and at least two identified peptides per protein and at least 4 fragments per precursor using R (4.1.3). Finally, LFQ values calculated using the DIA-NN R-package. Afterwards, analysis of results was performed in Perseus 1.6.15.[69]

Quantification of AA

For quantitative analysis of intracellular AA, T cells were treated with IMQ overnight. Then, cells were washed twice with ice-cold PBS. Dry pellets were snap-frozen and stored at -80°C. For extraction of metabolites from human skin samples, 4-mm punch biopsies were collected and immediately stored in PBS at 4°C. Samples were wrapped in 20uM Nylon mesh. The wrap was centrifuged and the flow-through was diluted with super cold Methanol. Supernatants were collected and stored at -80°C.

Endogenous AA were derivatized with benzoyl chloride and analyzed by Liquid Chromatography coupled to Electrospray Ionization Tandem Mass Spectrometry (LC-ESI-MS/MS) using a procedure previously described[70] with several modifications: One million frozen T cells were homogenized in 200 μl of acetonitrile/water 4:1 (v/v, pre-cooled at -20 °C) using the Precellys 24 Homogenisator at 6,400 rpm (twice 10 sec with 5 sec break) and directly put on ice again. Between 60 and 90 μl of tissue fluids were diluted with 100 μl of pre-cooled acetonitrile/methanol/water 2:2:1 (v/v/v). After centrifugation (16,100 RCF, 10 min, 4 °C), 20 μl of the supernatant were mixed with 10 μl of the MassChrom Internal Standard Mixture Amino acids and Acylcarnitines from Dried Blood (Chromsystems, Gräfelfing, Germany), reconstituted in 5 ml water/methanol 2:1 (v/v). Endogenous and isotope-labeled AA were derivatized by adding 10 μl of freshly prepared 2 % benzoyl chloride in acetonitrile and 10 μl of 100 mM sodium carbonate in water and thorough mixing. After addition of 50 μl of Milli-Q water and centrifugation (16,100 RCF, 5 min, 4°C), 80 μl of the supernatant were transferred to autoinjector vials.[70]

LC-MS/MS analysis was performed by injection of 5 μl of sample onto a Core-Shell Kinetex C18 column (100 mm × 2·1 mm ID, 2·6 μm particle size, 100 Å pore size, Phenomenex) and detection using a QTRAP 6500 triple quadrupole/linear ion trap mass spectrometer (SCIEX). The LC (Nexera X2 UHPLC System, Shimadzu) was operated at 30°C and at a flow rate of 0·4 ml/min with a mobile phase of 10 mM ammonium formate and 0·15 % formic acid in water (solvent A) and acetonitrile (solvent B). Benzoylated AA were eluted with the following gradient: initial, 0 % B; 0·01 min, 15 % B; 0·5 min, 17 % B; 14 min, 55 % B; 14·5 min, 100 % B; 16·5 min, 100 % B; 16.6 min, 0 % B; and 20 min, 0 % B. Benzoylated endogenous and isotope-labeled AA were monitored in the positive ion mode using their specific Multiple Reaction Monitoring (MRM) transitions. The instrument settings for nebulizer gas (Gas 1), turbogas (Gas 2), curtain gas, and collision gas were 50 psi, 70 psi, 40 psi, and medium, respectively. The Turbo V ESI source temperature was 500°C, and the ionspray voltage was 5·5 kV. For all MRM transitions the values for declustering potential, entrance potential, and cell exit potential were 80 V, 10 V, and 10 V, respectively. The collision energies ranged from 10 to 30 V.[70]

The LC chromatogram peaks of benzoylated endogenous and isotope-labeled AA were integrated using the MultiQuant 3.0.2 software (SCIEX). Intracellular AA were quantified by normalizing their peak areas to those of the internal standards (area ratio). For analyzing AA in tissue fluids, the area ratios of all AA of the respective sample were summed up. This sum was set equal to 100% and the proportion of each individual AA in this 100% was calculated.

CellPress
OPEN ACCESS

QUANTIFICATION AND STATISTICAL ANALYSIS

Statistical analysis

For proteomics experiments, statistical analyses were performed using Perseus 1.6.15.[69] Significantly regulated proteins were determined by Student's t-test on static p-value. All other statistical analysis was performed using Prism 10.1.2 software (GraphPad) and results are represented as mean +/- SEM. In case of strong donor inter-individual differences in raw values, values were normalized to control cells for analysis. *P*-values were calculated using two-tailed Student's *t*-tests. In some cases, as indicated in figure legends, measured values were log transformed to align data points to normal distribution. * $p<0{\cdot}05$, ** $p<0{\cdot}01$, *** $p<0{\cdot}001$. *n* refers to the number of biological replicates.